Lithos 202–203 (2014) 283–299

Contents lists available at ScienceDirect

Lithos

journal homepage: www.elsevier.com/locate/lithos

Subcontinental rift initiation and ocean-continent transitional setting of the Dinarides and Vardar zone: Evidence from the Krivaja–Konjuh Massif, Bosnia and Herzegovina

Ulrich H. Faul [a,*], Gordana Garapić [b,3], Boško Lugović [c,1,2]

[a] Earth, Atmospheric and Planetary Sciences, Massachusetts Institute of Technology, Cambridge, MA, USA
[b] Department of Earth Science, University of California, Santa Barbara, Santa Barbara, CA, USA
[c] Department of Mineralogy, Petrology and Mineral Resources, University of Zagreb, Zagreb, Croatia

ARTICLE INFO

Article history:
Received 21 February 2014
Accepted 24 May 2014
Available online 4 June 2014

Keywords:
Balkan ophiolites
Subcontinental lithosphere
Rift initiation
Ocean continent transition
Melt migration
Deformation

ABSTRACT

The Dinaride and Vardar zone ophiolite belts extend from the south-eastern margins of the Alps to the Albanian and Greek ophiolites. Detailed sampling of the Krivaja–Konjuh massif, one of the largest massifs in the Dinaride belt, reveals fertile compositions and an extensive record of deformation at spinel peridotite facies conditions. High Na_2O clinopyroxene and spinel–orthopyroxene symplectites after garnet indicate a relatively high pressure, subcontinental origin of the southern and western part of Krivaja, similar to orogenic massifs such as Lherz, Ronda and the Eastern Central Alpine peridotites. Clinopyroxene and spinel compositions from Konjuh show similarities with fertile abyssal peridotite. In the central parts of the massif the spinel lherzolites contain locally abundant patches of plagioclase, indicating impregnation by melt. The migrating melt was orthopyroxene undersaturated, locally converting the peridotites to massive olivine-rich troctolites. Massive gabbros and more evolved gabbro veins cross-cutting peridotites indicate continued melt production at depth. Overall we infer that the massif represents the onset of rifting and early stages of formation of a new ocean basin. In the south of Krivaja very localized chromitite occurrences indicate that much more depleted melts with supra-subduction affinity traversed the massif that have no genetic relationship with the peridotites. This indicates that volcanics with supra-subduction affinity at the margins of the Krivaja–Konjuh massif record separate processes during closure of the ocean basin. Comparison with published compositional data from other Balkan massifs shows that the range of compositions within the Krivaja–Konjuh massif is similar to the compositional range of the western massifs of the Dinarides. The compositions of the Balkan massifs show a west to east gradient, ranging from subcontinental on the western side of the Dinarides to depleted mid-ocean ridge/arc compositions in the Vardar zone in the east. This is consistent with the hypothesis that both ophiolite belts originate in a single ocean, rather than from two separate basins. A distinct decrease in fertility occurs in the south of the Dinarides towards the Albanian ophiolites with supra-subduction affinity.

1. Introduction

The Dinaride ophiolite belt together with the peridotites of the Vardar Zone Western Belt are part of the Alpine–Himalayan suture zone of the former (Neo-)Tethys ocean that separated Gondwana and Eurasia during the Mesozoic (e.g. Dilek and Furnes, 2011; Hrvatović and Pamić, 2005; Karamata, 2006; Pamić et al., 2002; Robertson et al., 2009, and references therein). These two belts, together with the Main Vardar Belt (Karamata, 2006; Robertson et al., 2009, see Section 6 for further discussion of the tectonic units) to the east provide the link between the Alpine peridotites to the north-west and the Albanian and Greek peridotites (Hellenides, e.g. Smith, 1993) to the south (Fig. 1).

The Krivaja–Konjuh massif in central Bosnia is one of the largest complexes within the Dinaride ophiolite belt with an area of ~650 km^2 (Fig. 2, Pamić et al., 2002; Bazylev et al., 2009). For comparison, the Ronda massif in southern Spain has an area of about 300 km^2 (Soustelle et al., 2009). The massif itself is considered to consist of two parts, separated by a major northwest–southeast trending fault. This fault is inferred to juxtapose a more fertile western part (Krivaja) and a more depleted eastern part (Konjuh). Different inferences exist for the tectonic setting of the massif as a whole, and whether the two parts originate in different settings. Based on the geochemistry of a few samples, the relatively fertile peridotites from the Krivaja have

* Corresponding author at: Dept. of Earth, Atmospheric and Planetary Sciences, 54-714, Massachusetts Institute of Technology, 77 Massachusetts Avenue, Cambridge, MA 02139-4307.
E-mail address: hufaul@mit.edu (U.H. Faul).
[1] Formerly at.
[2] Deceased 12 May 2013.
[3] Now at: Department of Geological Sciences, SUNY New Paltz, NY, USA.

http://dx.doi.org/10.1016/j.lithos.2014.05.026
0024-4937/

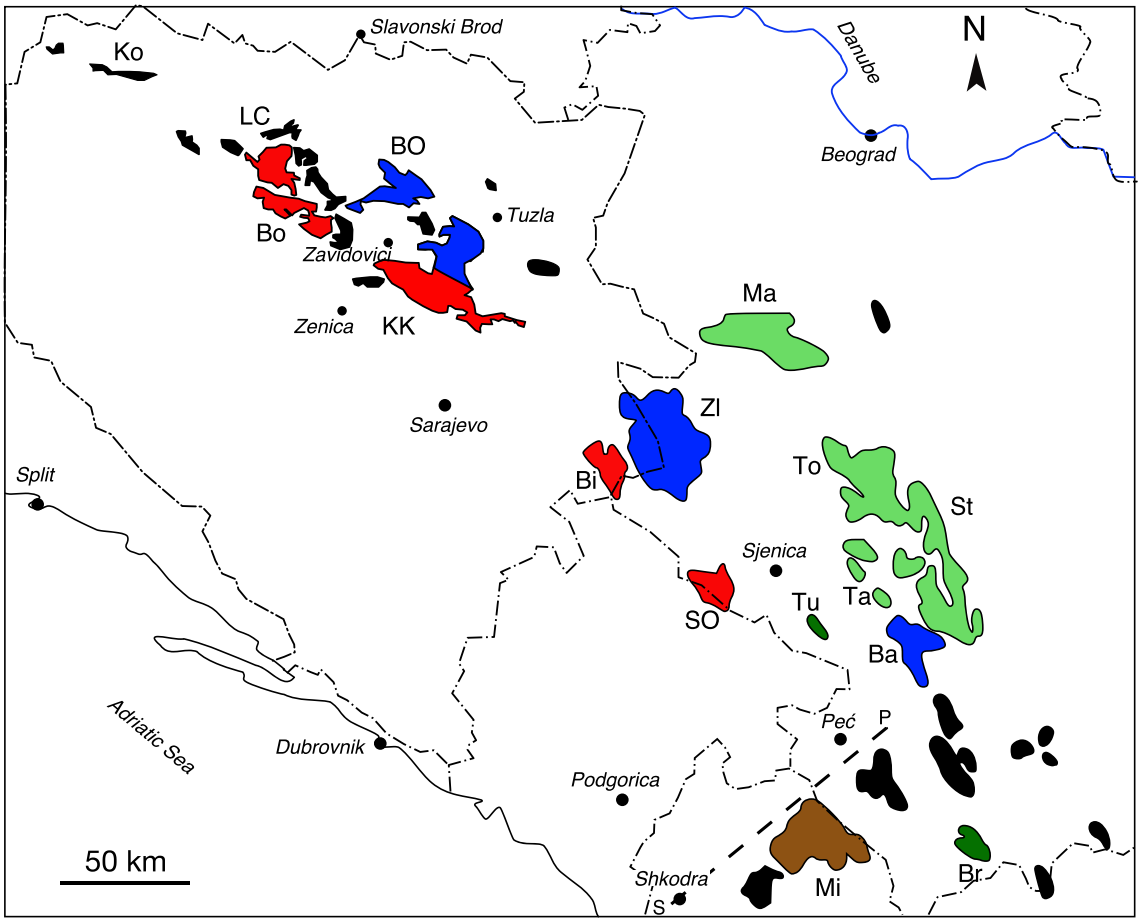

Fig. 1. Overview of the Balkan peridotite massifs (after Lugović et al., 1991; Ustaszewski et al., 2010). *Dinarides*: Ko, Kozara; LC, Ljubić–Čavka; BO, Bosanski Ozren; Bo, Borja; KK, Krivaja–Konjuh; Zl, Zlatibor; Bi, Bistrica; SO, Sjenički Ozren; Tu, Tuzinje. textitVardar Zone: Ma, Maljen; To, Troglav; St, Stolovi (Ibar); Ta, Trnava; Ba, Banjska. *Albanide–Hellenides*: Mi, Mirdita; Br, Brezovica. S P: Skutari-Peć line. Colors correspond to compositions in Fig. 10, indicating west to east depletion. (For interpretation of the references to color in this figure legend, the reader is referred to the web version of this article.)

been associated with either subcontinental lithosphere or a mid-ocean ridge setting (Bazylev et al., 2009; Lugović et al., 1991; Robertson et al., 2009), but a back-arc basin setting has also been inferred for the Konjuh (Lugović et al., 2006; Pamić et al., 2002, and references therein). Volcanics found at the margins of the massif as well as in the ophiolitic mélange nearby that have arc/back-arc signatures complicate the interpretation (Lugović et al., 2006; Robertson et al., 2009).

The field observations and analyses described in this manuscript are predominantly from Krivaja, although some samples were also collected from Konjuh (Fig. 2). The field observations indicate that the peridotites were exhumed in a magma-poor ocean floor setting, while microstructural observations and mineral chemistry indicate a fertile, subcontinental origin, consistent with inferences from the fertile nature of many of the Dinaride massifs (Bazylev et al., 2009; Lugović et al., 1991). The compositions of some of the south-eastern parts of the Krivaja and from parts of the Konjuh are somewhat more depleted, with mid-ocean ridge (MOR) affinity. Despite the near complete absence of harzburgites and dunites, the massif contains an extensive record of melt migration that culminates in olivine-rich troctolites. These will be described in more detail separately.

2. Geologic setting

The Krivaja–Konjuh peridotite massif is embedded in an ophiolitic mélange with a matrix of fine-grained sedimentary origin. The mélange contains fragments of ultramafic, mafic intrusive and volcanic rocks, as well as limestones and cherts (indicating a deep water origin) with a range of ages (see e.g. Pamić et al., 2002; Robertson et al., 2009, and references therein for more details). The massif is surrounded by smaller ultramafic bodies, with the nearest larger one about 20 km to the north (Fig. 1, Bosanski Ozren, with an area of ~300 km^2).

The massif is partially bordered by Triassic and Jurassic limestone. We examined the contact between peridotite and Triassic limestone in a limestone quarry in the north-western corner of the massif (Fig. 2). This contact showed only minor calcite veins extending from the limestone into the overlying completely serpentinized peridotite, indicating relatively low temperatures on contact between the two units.

Parts of the southern margin of the Krivaja are bounded by a metamorphic sole, grading from greenschist-facies in its lowermost parts to amphibolite–granulite-facies towards the contact with the peridotites (Pamić et al., 2002). The pressure estimates range up to 1 GPa at temperatures between 620 and 830 °C (Operta et al., 2003). The contact between metamorphic sole and ophiolitic mélange is described as of tectonic origin (Operta et al., 2003). Ages obtained by K–Ar dating of amphibolites range from 157 to 170 Ma (Pamić et al., 2002), although a Sm–Nd isochron from peridotites from three different massifs suggests a younger age of 136 Myr (Lugović et al., 1991).

The division into separate sections (Krivaja in the west and Konjuh in the east) is in part based on the occurrence of a major fault zone that can be traced from the northwest to the southeast through the massif. We examined the fault zone in three areas (Džinica, Dištica and Vojnica, Fig. 2). The fault zone and adjacent rocks are completely serpentinized, blocky at Dištica and reduced to a microbreccia in Vojnica

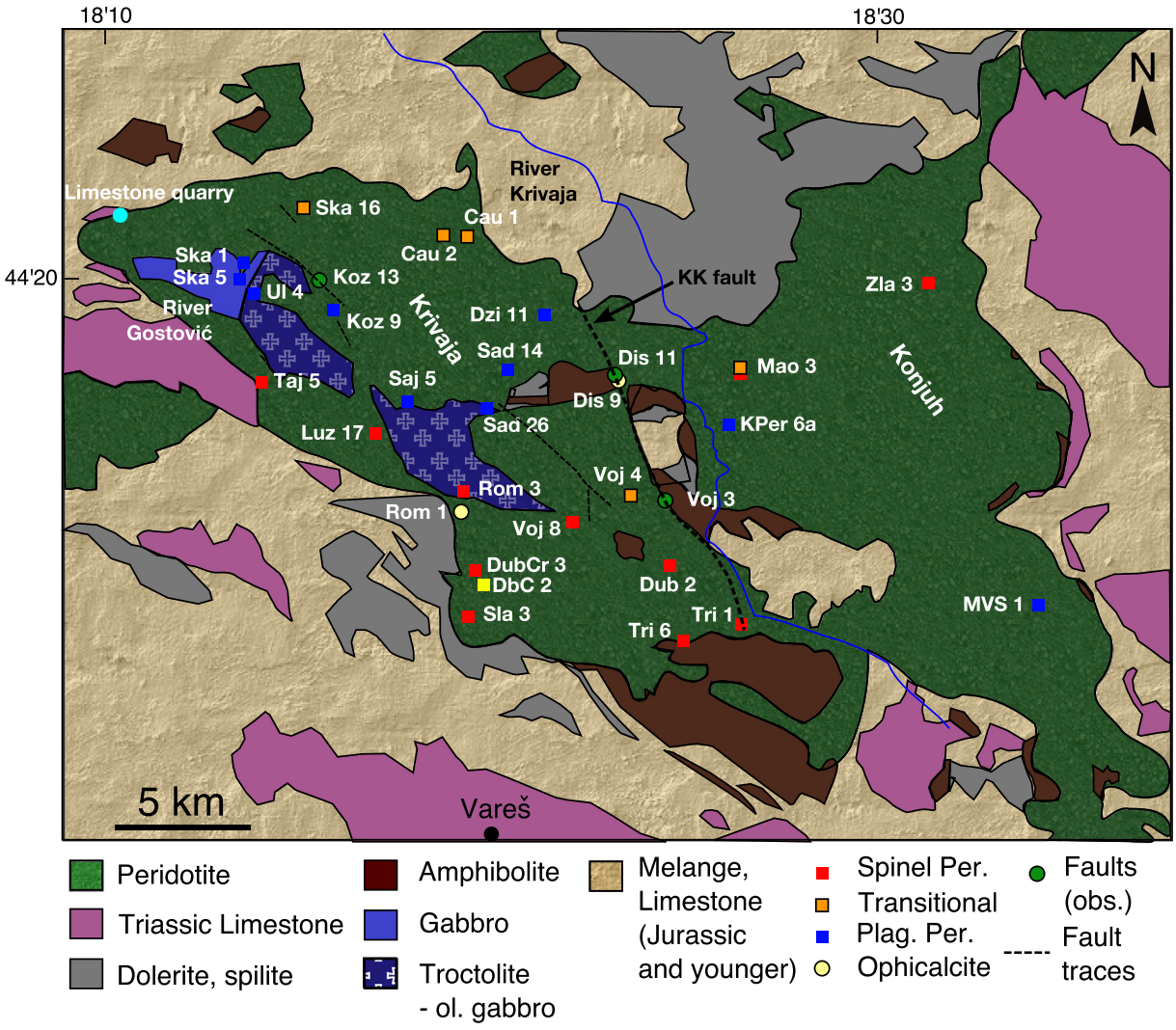

Fig. 2. Simplified geological map of the Krivaja–Konjuh massif with sample locations indicated. The map was constructed from four sheets of geologic maps of the former Yugoslavia (Zavidovići, Tuzla, Vlasenica, Vareš, Federal Geological Institute, 1971–1990). Sample locations marked in red represent spinel peridotites, orange transitional, blue are plagioclase peridotites (see text). Major faults are represented by dashed lines, the location of pictures shown in Fig. 3 are shown by green dots. Not all faults are shown. The fault separating the Krivaja portion to the west from the Konjuh portion to the east is indicated. The extent of gabbro and troctolite outcrops are approximate, both tend to occur together and are interlayered with peridotite at the margins. (For interpretation of the references to color in this figure legend, the reader is referred to the web version of this article.)

(Fig. 3a) and Džinica. In all locations the fault rocks appear to be of mantle origin, with no indications of intercalated crustal lithologies. Similar relatively well developed serpentinized shear zones also occur elsewhere in the massif (Fig. 3b).

In some cases fault zones within the massif and near the main Krivaja–Konjuh fault are associated with ophicalcites (Fig. 3d), where limestone is in conformable contact with and contains brecciated fragments of serpentine or gabbro. The breccias do not include sandstone and show no evidence of prior transport of clasts, in contrast for example to observation from Lherz (Lagabrielle and Bodinier, 2008). Boulders from watercourses that are entirely within the massif similarly show conformable contacts between peridotite and limestone or chert (Fig. 3c). A deep water origin is also indicated by minor pillow basalts and cherts observed in the central-western part, although the structural relationship of these outcrops with the surrounding peridotites is not easy to ascertain.

The surface carbonation reactions described by Kelemen and Matter (2008) in a desert environment with low erosion rates produce sets of expansion joints, as shown in their Fig. 1. In contrast, the carbonates and ophicalcites in the Krivaja are found in incised stream beds with high erosion rates; they are associated with faults and shear deformation structures rather than inflation (expansion) structures. Carbonate veins in a joint patterns have also not been observed in weathered outcrops away from stream beds. Based on the structural observations we therefore infer that the ophicalcites in this massif are not due to recent surface carbonation reactions.

3. Peridotites

3.1. Overview

Samples were collected from all parts of Krivaja, as well as four locations from Konjuh (see Fig. 2 and Table 1 for place names and locations). The freshest samples were typically found along stream beds, which also provided relatively convenient access. The choice of samples for analysis was based on coverage of the massif as well as freshness. Whenever possible samples from outcrop were chosen for analysis, but in some cases boulders collected in stream beds (from relatively small tributary streams wholly within the massif) were fresher. All samples were affected by serpentinization, introducing uncertainties in

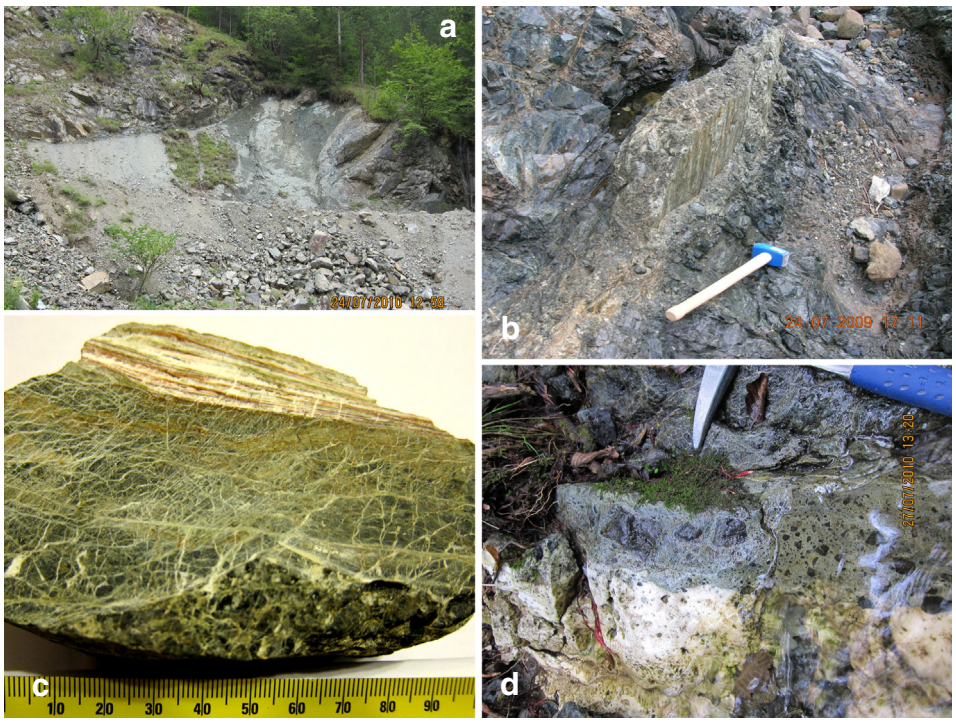

Fig. 3. Examples of faults and shear zones from Krivaja–Konjuh. (a) Outcrop of the Krivaja–Konjuh fault at Vojnica. The shear zone material consists of microbrecciated serpentine. Adjacent rocks are also completely serpentinized. Field examination suggests that the serpentinized rocks in the shear zone are of mantle origin, rather than a melange, or mafic rocks. (b) Outcrop of a serpentinized fault at Kozjak. (c) Limestone and chert layers atop serpentinized peridotite at Romanovac. (d) Limestone containing serpentinite fragments adjacent to serpentinite breccia in an outcrop in Dištica. The larger fragments in the breccia consist of serpentinized peridotite. The outcrop is located near the Krivaja–Konjuh fault and at the border between peridotite and amphibolite.

analysis, point counting of modes and grain size determination from thin sections. Grain sizes and deformation intensity vary locally, the grain sizes given below are intended to be representative for a given locality. Particularly the rocks in faults and shear zones are almost always completely serpentinized and in some instances further altered to talc and clay, making identification of the original lithology difficult in the field. An overview over the samples analyzed is given in Table 1, the sample locations are shown in Fig. 2.

The Krivaja–Konjuh massif consists of spinel and plagioclase peridotites as well as massive troctolites and gabbros. The peridotites consist of lherzolites with clinopyroxene (cpx) contents from just above 5% ranging up to 15%. Rocks that can be classified as dunite or harzburgite based on mineral mode are volumetrically very minor and typically contain one or a combination of cpx, plagioclase and spinel with interstitial geometries. The sparsity of dunites in the Krivaja–Konjuh massif is similar to their near complete absence in the Dinarides overall (Lugović et al., 1991).

Spinel and plagioclase lherzolites occur both in Krivaja and Konjuh. The western and southern parts of Krivaja, bounded to the north and east by the massive troctolites, consist of spinel peridotites (Fig. 2). In Konjuh spinel peridotites are found in the north-eastern part (Zlaća). The spinel peridotites show no signs of re-equilibration in the plagioclase stability field. Plagioclase peridotites occur to the north and east of the troctolites in Krivaja, and the center and south of Konjuh.

The lithologies in the central-western portion of the Krivaja shown as troctolites and gabbros in Fig. 2 range from massive olivine-rich troctolites to troctolites, olivine gabbros and gabbros. The adjacent peridotites are intruded by gabbro veins and dikes ranging from mm to m scale (Fig. 4a–c), with diffuse (relatively high temperature) to sharp sided (lower temperature) contacts with the host rock. Cross-cutting relationships between the gabbro veins indicate at least three generations in some locations, with the latest generation appearing the most evolved, with near pegmatitic domains (Fig. 4c). Thin, cross cutting gabbro veins as well as thicker anastomosing veins occur occasionally in all parts of the massif where plagioclase is observed.

Locally abundant gabbro veins as well as outcrop-scale variable proportions of plagioclase patches and veinlets occur in Stara Kamenica (Ska1, 5). The very heterogeneous lithologies range from dunitic patches, to harzburgitic to essentially gabbroic compositions (Fig. 4e). Variable lithologies including small (10–20 cm sized) dunite patches also occur in Kozjak (Koz9), Sadjevica (Sad14) and in Maoča (Konjuh).

Clinopyroxene-rich pyroxenite patches, veins and layers occur in Sadjevica. The pyroxenites are parallel to the foliation, which is expressed by the alignment of somewhat elongate orthopyroxene (opx) grains (Fig. 4b). In one location pyroxenite veins appear to be gently folded and somewhat boudinaged. Relatively thin pyroxenite veins/layers occur throughout the massif (e.g. Dištica, Vojnica, Duboštica, Tribija, Maoča). In Vojnica and similarly in Muška Voda in Konjuh more opx-rich layers occur at a small angle to the foliation.

Chromite mines have been mapped in the south of the Krivaja by the Federal Geological Institute of Yugoslavia (Federal Geological Institute, 1971–1990). The largest mine site near Duboštica is accessible and contains abundant chromitite fragments in the vicinity of the mine entrance. The peridotites immediately surrounding the mine are heavily serpentinized, however. Outcrop of peridotite at a distance of about 150 m from the mine entrance, while still partially altered is very fertile (see below), spinel rich (>3%) spinel peridotite, and typically highly deformed.

3.2. Microstructures

The peridotites throughout the massif record a high grade of deformation and associated recrystallization. The deformation grade of the spinel peridotites in Krivaja is on average higher than in Konjuh. The largest remaining porphyroclasts of olivine and orthopyroxene

Table 1
Sample locations[a], outcrop and thin section notes.

Sample number	Location	T, opx °C[c]	Notes
Krivaja			
	Limestone quarry		Contact between Triassic limestone and peridotite (serp.)
Ska1	St. Kamenica		PL; anastomosing veins of coarse ol gab., ol fg, euhedral, plag interstitial, up to 5% magnetite.
Ska5	St. Kamenica		Multiple episodes of melt migration: PL, fg; plag dunite/troct. very fg; sp; plag interstitial.
Ska16	St. Kamenica		Trans.; mg porph., part. mosaic, plag patches (interstitial)//ol elongation, dismembered ol
Ul4	Ulen		PL; opx porph., elongate, foliated; ol recrystallized more fine-grained; little spinel
Cau1	Čauševac	1180	Trans.; large lobate ol w. subgrain bd, ol matrix mosaic texture; plag interstitial, undeformed; dark brown sp
Cau2	Čauševac		Boulder w. PL — gabbro contact, PL layered w. coarse and fine ol, coarse opx, porph. brown sp. mantled with plag
Koz9	Kozjak		Contact troct.-PL. PL has coarse, el. porph. + fg. ol; opx: corroded gb, exsolved cpx, ol; plag interstitial; troct.: plag trails, minor elongate opx
Koz13	Kozjak		Shear zone, gabbro peridotite
Luz17	Lužnica	960	SL; mg porph.; coarse, dark brown sp + fine light brown sp
Taj5	Tajašnica		SL; cg porph., elongate ol (sgb), + fg matrix; sp-opx intergrowths (rounded); fg. sp
Saj5	Sajavica	1060	PL, all ol fg; opx and cpx porph., ol included in opx; dark brown sp rimmed w. plag + opx.
Sad14	Sadjevica		PL; mg. porph., dunite patch
Sad26	Sadjevica	1080	PL, mg.; ol porph. + fg matrix; plag patches; no sp
Dzi11	Džinica	1010	PL, ol mg. mosaic, few porph.; plag patches; sp rimmed w. plag + opx (undeformed).
Dis9	Dištica		Contact amphibolite–peridotite; limestone
Dis11	Dištica		KK fault, serpentinized, blocky
Rom1	Romanovac		Ophicalcite.
Rom3	Romanovac		SL; mg; thin gabbro veins; sp light brown fg.
Voj3	Vojnica		KK fault, serpentinized, granular.
Voj4	Vojnica		Trans.; mylonitic, coarse spinel rimmed by plag.
Voj8	Vojnica		SL; mylonitic, some elongate opx (20:1),>1 cm.
Dub2	Duboštica		SL; ol largest porph., undulose extinction; opx porph. elong. corroded gb.; sp light brown, fg, opx intergrowth.
DubCr3	Duboštica	890	SL; (ultra-) mylonitic, fine spinel trails. ~350 m from chromite mine/chromitites.
DbC2	Duboštica		Chromitite from main chromite mine with attached silicates containing fresh cpx. Massive sp dark brown.
d18[b]	Duboštica		Chromitite from chromite mine
Sla3	Slani Potok		SL; light brown sp trails//elongate ol proph.
Tri1	Tribija		SL; porph.; ol mg elongate, ol included in opx.
Tri6a	Tribija		SL; layered peridotite–pyroxenite. Deformd, per. more fg some larger opx porph in per.; light brown elongate sp.
Konjuh			
MVS1[b]	Muška Voda		PL; mg.
KPer6a	R. Krivaja		PL; mg porph, interstitial. plag.
Mao3[b]	Maoča		SL, Trans.; dark brown sp, interstitial. plag.
Zla3[b]	Zlaća		SL; cg–mg porph.

Abbreviations. PL, SL: plagioclase, spinel lherzolite; Trans.: Transitional PL–SL; ol: olivine; sp: spinel; plag: pladioclase; fg, mg, cg: fine, medium, coarse grained; mosaic indicates recovery/grain growth after deformation; porph.: porphyroclastic; troct.: olivine troctolite consisting of 80–90% olivine, plagioclase and sometimes minor opx, cpx, spinel; sgb: subgrain boundaries.
[a] See Fig. 2, and Table 3 for GPS coordinates.
[b] Analyses from Šegvić (2010).
[c] Temperature estimates based on the Ca-in-opx thermometer of Brey and Köhler (1990) (thin section averages).

range in size from 3 to 5 mm, suggesting that this may have been the grain size before deformation of the peridotite (Fig. 5a). Olivine is frequently recrystallized, occasionally to grain sizes <100 μm (Fig. 5b). Remaining olivine porphyroclasts are elongate with parallel subgrain walls showing undulose extinction (Fig. 5a, d). Dismembered grains can be identified by their simultaneous extinction. Based on the degree of recrystallization the microstructures can be characterized as ranging from protomylonitic (with an olivine mean grain size of ~0.7 mm, Duboštica) to mylonitic–ultramylonitic (mean grain size of 0.3 mm, Vojnica; to 0.1 mm, Sajavica).

Coarse, undeformed symplectites of opx and spinel occur in the western-most part (Tajašnica, Fig. 5e). Garnet-shaped spinel–opx–plagioclase intergrowths also occur in Sajavica (Fig. 5f). Deformation of the coarse symplectites resulted in vermicular spinel grains interstitial to opx neoblasts (Fig. 5c). No symplectites remain in mylonites and ultramylonites (Fig. 5b), which contain ribbons of nearly touching, fine-grained light brown (interstitial) spinels that extend across individual thin sections. The highly deformed spinel peridotites show no signs of recovery and grain growth after deformation, indicating that temperatures remained relatively low during exhumation. Porphyroclastic, dark brown and fine-grained, light brown spinel coexists in the central-western part (Lužnica) as well as the southern part (Duboštica) of the massif.

In the spinel peridotites orthopyroxene frequently occurs as porphyroclasts with exsolution lamellae, occasionally showing extreme elongation with aspect ratios >10:1 (Taj5, Voj8, Fig. 5b). Locally it is

Fig. 4. Outcrop-scale features representing melt migration. (a) Anastomosing gabbro veins surrounding blocks of peridotite (Stara Kamenica). (b) Olivine-gabbro vein cross-cutting foliation in peridotite. The foliation is marked byopx porphyroclasts, with foliation-parallel pyroxenite layers and lenses (Sadjevica). (c) Intrusion of three generations of gabbro veins into plagioclase peridotite near the contact with massive gabbro units. The gabbro compositions range from olivine-rich to evolved-pegmatitic (Stara Kamenica). (d) Peridotite strongly modified by migrating melts. The darkest brown colors indicate plagioclase–dunite compositions, lighter brown are remnants of the original lherzolite, more plagioclase-rich portions are white. (For interpretation of the references to color in this figure legend, the reader is referred to the web version of this article.)

alsocompletely recrystallized to fine grain sizes, giving the rock a smooth appearance on weathered surfaces. Clinopyroxene ranges from porphyroclastic (particularly the spinel peridotites in Zlaća, also Vojnica) to completely recrystallized (e.g. the spinel peridotites in Duboštica).

By contrast microstructures in the plagioclase peridotites show onset of recovery after deformation. Olivine is on average relatively fine-grained (e.g. 0.6 mm, Čauševac), but the size difference between large and small grains is not as pronounced as in the spinel peridotites. Elongate porphyroclasts with subgrain boundaries still occur, but they have largely smooth grain boundaries (Fig. 6a, b). Smaller grains tend to have more euhedral shapes, indicating grain growth after deformation. Plagioclase in these rocks occurs as interstitial patches or ribbons (Fig. 6c), which are aligned parallel to the foliation where it is observable. Plagioclase also occurs as reaction rims around spinel (e.g. Fig. 6b). Significantly, plagioclase, whether in the form of overgrowths around spinel or interstitial patches shows no sign of deformation. Similarly opx porphyroclasts, in the process of being replaced by cpx and olivine (Fig. 6d) show no signs of deformation. Cpx in the plagioclase peridotites occurs as porphyroclasts or grains with interstitial shapes but with an overall lower mode compared to spinel peridotites.

4. Compositions

4.1. Analytical procedures

Microprobe analyses were performed at the MIT Electron Microprobe Facility on both the JEOL-JXA-8200 and JEOL-JXA-733 with 15 kV acceleration potential and a beam current of 10 nA and a beam diameter of ~1 μm. Counting times were 20–40 s per element, resulting in counting precisions of 0.5–1.0% 1-sigma standard deviations. The raw data were corrected for matrix effects with the CITZAF program (Armstrong, 1995). Additional microprobe analyses were performed at the Research School of Earth Sciences, Australian National University, using a Cameca SX-100 electron microprobe operating at 15 kV and a beam current of 20 nA. Standards were analyzed before and during each session with 1-sigma standard deviations <0.5%. The same analytical protocol was used for all minerals on each probe. Typically one thin section was analyzed from each locality for all the phases present. Except for Ca contents in opx for the thermometer of Brey and Köhler (1990) the compositions were not averaged. Plagioclase is commonly altered, and is not reported here. Compositional ranges are shown in Table 2, the complete dataset is included as supplementary material.

4.2. Mineral chemistry

4.2.1. Olivine

Overall the compositions of the peridotites are moderately depleted relative to MORB source mantle (e.g. DMM, Workman and Hart , 2005). This is expressed by an average olivine Mg# of 90.2 with a range between 89.3 and 91.1 for Krivaja (c.f. DMM 89.5, see supplementary Table). Although each location shows some variability, peridotites from the southeast in Krivaja tend to be at the depleted end with the highest Mg# (e.g. Tribija, Vojnica), while the plagioclase peridotites from the northern part tend to have the lowest Mg# (e.g. Sajavica). Olivines from Konjuh show the same narrow range in Mg#, with an average near Mg# 90 (Šegvić, 2010). Interstitial olivine in the chromitites has significantly higher Mg# than all other rocks, from 91.6 to above 92.2 (Šegvić, 2010).

4.2.2. Orthopyroxene

Large, porphyroclastic opx grains commonly show exsolution lamellae and internal deformation features in the spinel peridotites

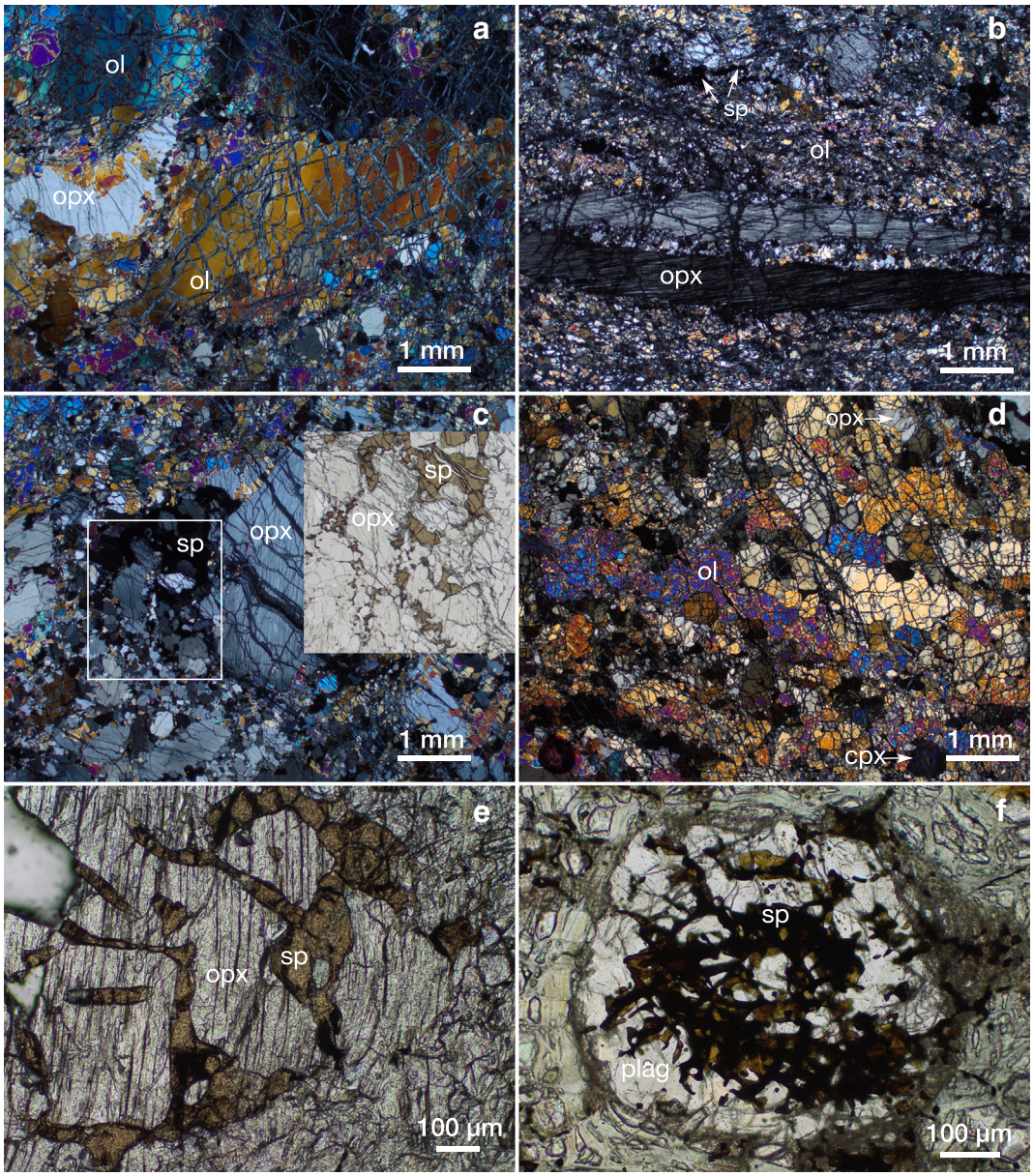

Fig. 5. Spinel peridotite microstructures. (a) Spinel lherzolite near Duboštica showing the largest remaining olivine porphyroclasts in Krivaja, characterized by undulose extinction (Dub2). (b) Mylonitic microstructure with elongate opx porphyroclasts. Olivine is completely recrystallized (Voj8). (c) Incipient recrystallization of coarse opx-spinel symplectite and an opx porphyroclast. The inset shows that the recrystallized parts of the coarse spinel become interstitial to opx neoblasts (Dub2). (d) Elongate and partially dismembered olivine grains. Opx is recrystallized in this sample (Taj5). (e) Coarse intergrowth of spinel and orthopyroxene, suggesting a garnet origin (Tajašnica, Piccardo et al., 2007). (f) Spinel, plagioclase and orthopyroxene in the shape of a garnet crystal in Sajavica. Fluid inclusions are also present. The pseudomorph is surrounded by an alteration rim. While the olivine grain size is reduced to 0.1 mm in this area, the spinel intergrowths appear undeformed.

(Fig. 5b, c). In the transitional and plagioclase peridotites, besides internal deformation, opx porphyroclasts also show signs of reaction with other phases (Fig. 6c, d). Correspondingly, the compositions show a wide range within individual grains and thin sections (Supplementary table) and are not further discussed here. Particularly in the transitional peridotites large opx grains tend not to be in equilibrium with frequently smaller cpx grains, so that two-pyroxene thermometry does not yield useful temperature estimates. Thin section averages of CaO in opx were used for temperature estimates for individual localities with the Brey and Köhler (1990) thermometer.

4.2.3. Clinopyroxene

With some scatter, cpx compositions from individual localities have distinct characteristics (see supplementary table). For the massif as a whole the most obvious feature is the difference in composition between plagioclase-bearing and plagioclase-free peridotites with regard to their Na_2O and Al_2O_3 contents (Fig. 7) (Supplementary Table). As a function of TiO_2 the spinel peridotites form a trend at Al_2O_3 contents between ~5 and 7 wt.% towards the model MORB source composition DMM (Workman and Hart, 2005) at the fertile end (Fig. 7a). Plagioclase peridotites form a similar trend but at lower Al_2O_3 contents due to the partitioning into plagioclase (Dick et al., 2010; Rampone et al., 1993). Peridotites from Čauševac, Stara Kamenica, and Maoča contain cpx grains with both high and low Al_2O_3 contents, straddling the two trends.

The Na_2O contents of cpx from the Krivaja spinel peridotites range to twice the value for DMM, and are consistently higher than those of the plagioclase-bearing peridotites (Fig. 7b). Overall the clinopyroxenes form a trend of moderately decreasing Al_2O_3 contents for a broad range

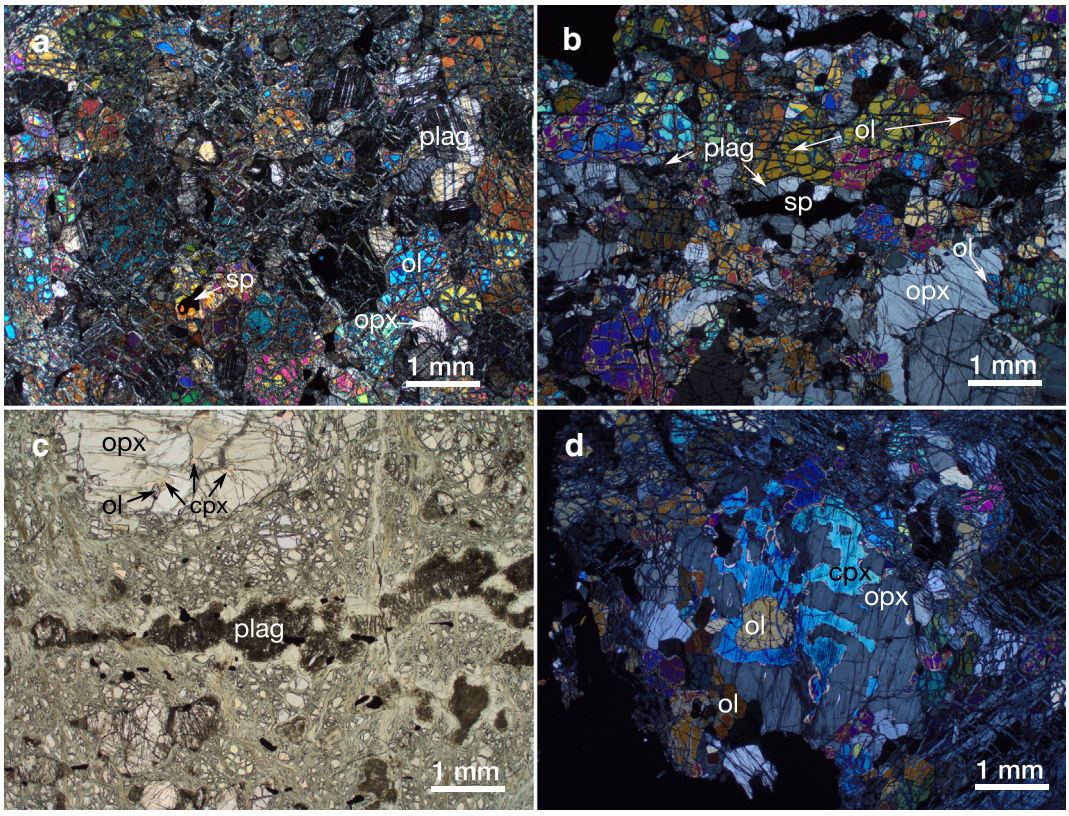

Fig. 6. Plagioclase peridotite microstructures. (a) Peridotite with interstitial and euhedral plagioclase grains. In comparison to the spinel peridotites the grain size is relatively uniform with no indication of deformation also in the plagioclase (Koz9). (b) Microstructure showing recovery from deformation. A previous high grade of deformation is evident in elongate and partially dismembered olivine grains, similar to the elongate grains in spinel peridotites (Fig. 5d). Black elongate patches in the center and top of the image are spinel grains surrounded by a rim of plagioclase grains. Interstitial plagioclase patches are also indicated. Opx grains are being replaced by olivine and cpx (Cau2). (c) Plane-polarized light image of ribbons and patches of (altered) plagioclase. The porphyroclastic orthopyroxene grain at the top of the image is partially replaced by clinopyroxene and olivine (Koz9). (d) Cross-polarized image of an opx grain that is being replaced by olivine and cpx (Koz9).

of Na_2O. With few exceptions, rocks from Konjuh form a steeper trend starting from Al_2O_3 contents as high as Krivaja, but at Na_2O below 1%. The highest Al_2O_3 and Na_2O contents in Fig. 7 come from a pyroxenite vein in sample Tri6a. Cpx compositions outside of the vein in the same thin section are similar to other spinel peridotites. Cpx compositions in the chromitites from Duboštica are significantly more depleted in Al_2O_3 and TiO_2 than in any other rocks from the massif, but they do have somewhat elevated Na_2O contents.

4.2.4. Spinel

Spinel compositions from Krivaja–Konjuh peridotites form the same groupings as cpx compositions (Fig. 8). Spinel peridotites from

Table 2
Compositional ranges, wt.%.

Oxide wt.%	SiO_2	TiO_2	Al_2O_3	Cr_2O_3	FeO	MnO	MgO	CaO	NiO	Na_2O
Plag. P										
Ol	39.6–41.3	–	–	–	9.5–10.3	0.11–0.19	48.8–51.0	–	0.31–0.48	
Opx	53.7–56.7	0.06–0.26	1.8–7.3	0.35–0.91	5.5–7.2	0.09–0.20	29.0–34.9	0.36–3.68	–	
Cpx	49.8–53.7	0.16–0.87	1.88–3.77	0.55–1.52	2.29–3.43	0.0–0.19	16.0–18.6	20.2–24.8	–	0.09–0.57
Sp	–	0.01–0.85	20.7–56.5	9.8–41.9	12.8–28.3	0.06–0.83	8.0–20.2		0–0.36	
Transitional										
Ol	39.6–41.3	–	–	–	8.8–10.1	0.03–0.21	49.3–51.2	–	0.33–0.44	
Opx	54.4–55.9	0.09–0.13	2.67–4.33	0.74–1.00	6.3–6.7	0.13–0.20	32.5–33.9	1.27–2.1	–	
Cpx	48.7–53.7	0.22–0.62	2.45–7.85	0.28–1.41	2.21–3.08	0.01–0.16	14.4–18.0	21.8–23.6	–	0.24–1.38
Sp	–	0.01–1.07	28.7–59.0	6.9–36.4	11.6–22.6	0.01–0.29	11.9–19.5		0.0–0.17	
Spinel P										
Ol	39.2–41.4	–	–	–	8.8–12.7	0.01–0.22	45.7–50.5	–	0.32–0.48	
Opx	53.6–57.1	0.05–0.18	2.89–6.44	0.04–0.57	6.20–8.19	0.14–0.30	31.7–33.68	0.31–1.07	–	
Cpx	50.1–54.8	0.16–0.61	2.46–8.89	0.05–1.31	2.11–4.94	0–0.18	13.5–18.4	17.5–23.7	–	0.42–2.62
Sp	–	0.01–0.11	48.8–62.5	7.3–19.1	10.8–14.4	0.0–0.31	17.9–20.1	–	0.0–0.44	
Chromitite										
Cpx	49.7–54.2	0.06–0.30	1.22–4.51	0.51–1.15	1.13–2.71	0.0–0.12	16.4–17.4	22.6–24.0	–	0.17–0.78
Sp	–	0.0–0.43	10.4–40.4	23.0–56.5	19.2–24.9	0.0–0.14	9.1–14.9	–	0.25–0.34	

Table 3
Sample locations.

Krivaja		
Limest. quarry	N44°21′37.5″	E18°09′32.0″
Ska1	N44°20′30.1″	E18°12′54.5″
Ska5	N44°20′24.6″	E18°12′51.2″
Ska16	N44°21′41.9″	E18°14′38.6″
Ul4	N44°20′2.2″	E18°12′59.0″
Cau1	N44°21′10.4″	E18°19′01.1″
Cau2	N44°21′13.1″	E18°18′15.3″
Koz9	N44°19′46.0″	E18°15′22.8″
Koz13	N44°20′01.4″	E18°15′25.9″
Luz17	N44°17′21.7″	E18°16′33.9″
Taj5	N44°18′23.0″	E18°13′27.8″
Saj5	N44°17′59.4″	E18°17′24.3″
Sad14	N44°18′35.4″	E18°20′09.7″
Sad26	N44°17′51.6″	E18°19′31.6″
Dzi11	N44°19′39.5″	E18°21′05.1″
Dis9	N44°18′24.3″	E18°23′00.8″
Dis11	N44°18′26.2″	E18°23′03.6″
Rom1	N44°15′53.6″	E18°18′47.6″
Rom3	N44°16′16.2″	E18°18′54.6″
Voj3	N44°16′01.3″	E18°24′15.6″
Voj8	N44°15′42.5″	E18°21′48.8″
Dub2	N44°15′11.1″	E18°24′46.2″
DubCr3	N44°14′45.5″	E18°19′13.8″
Chromite mine	N44°14′35.2″	E18°19′20.0″
Sla3	N44°13′52.8″	E18°19′02.7″
Tri1	N44°13′41.4″	E18°26′20.9″
Tri6a	N44°13′9.8″	E18°25′1.2″
Konjuh		
KPer6a	N44°17′30.8″	E18°25′26.7″
Muska Voda	N44°14′06.3″	E18°34′09.3″
Maoca	N44°18′39.4″	E18°26′16.9″
Zlaca	N44°20′15.5″	E18°31′21.5″

Parts of this area were affected by the Balkan war, local advice should be sought before visiting.

both parts have the lowest Cr# (=Cr/Cr + Al), highest Mg# (=Mg/Mg + Fe^{2+}), and the lowest TiO_2 contents (Supplementary Table). Cr# of plagioclase peridotites are significantly higher (0.4–0.6). Transitional peridotites have low and high Cr#-spinel in one thin section (e.g. Sajavica), but preserve the gap in compositions. The rocks show a similar gap in Mg# in a broad trend towards the lowest Mg# and highest Cr# of the plagioclase peridotites (Fig. 8b). A particular feature of the transitional and plagioclase peridotites is TiO_2 contents that extend to 1%. The compositions of chromitites from Duboštica in the south-western part of the massif are clearly distinct from the compositions of the rest of the massif, with much higher Cr# between 0.7 and 0.8. In contrast, spinel peridotites nearest to the chromitite mine site are among the most fertile in the massif with Cr# 0.1–0.15.

5. Discussion

5.1. Emplacement and exhumation

The near absence of contact metamorphism at the margins of both peridotite and metamorphic sole in contact with limestone implies that the massif was not far above ambient temperature during emplacement in its current location in the mélange. The high temperatures inferred for the metamorphic sole at the contact with the peridotites indicate that obduction of the peridotites onto the metamorphic sole predates inclusion into the mélange. High temperature records of deformation within the massif are therefore unrelated to tectonic emplacement of the massif in its current location.

Minor outcrops of chert together with pillow basalt interior to the massif indicate exposure on the ocean floor in a deep water environment. Exhumation and exposure of the peridotites to the ocean floor is also suggested by the conformable contact of limestone and chert layers on top of serpentinites criss-crossed by calcite veins (ophicalcite). Very minor occurrence of basalts indicates a magma-poor environment. The extensively serpentinized faults and shear zones interior to the massif are similar to faults observed for example at the slow-spreading Mid-Atlantic Ridge near the 15°20′ fracture zone (Schroeder et al., 2007), which accommodated exhumation of the peridotites to the seafloor. Overall the exhumation of the massif may be comparable to non-volcanic exhumation of peridotites at slow spreading ridges (e.g. Cannat, 1993; Schroeder et al., 2007) or continental margins (e.g. Rampone and Piccardo, 2000; Müntener et al., 2010), although further detailed examination of the shear zones, as well as the cherts, is needed to constrain their origin and significance. No signs of prograde metamorphism have been observed in gabbros or peridotites, indicating that following exhumation, the massif remained at low pressure.

5.2. Melt infiltration

The map of the Krivaja–Konjuh massif (Fig. 2) shows that plagioclase and transitional peridotites are wide-spread in both parts of the massif.

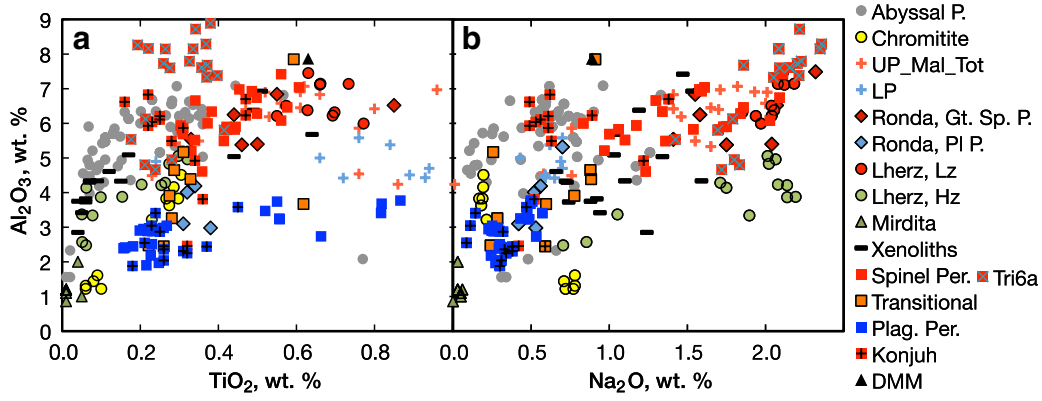

Fig. 7. Clinopyroxene compositions from the Krivaja–Konjuh massif (squares, this study and Šegvić , 2010) as well as other massifs, abyssal peridotites and xenoliths for comparison. (a) Al_2O_3 vs TiO_2 and (b) Al_2O_3 vs Na_2O. Plagioclase-free spinel peridotites are shown in red, plagioclase-bearing peridotites that contain cpx both high and low in Al_2O_3 in one thin section are orange (transitional samples), and apparently equilibrated plagioclase peridotites in blue. Sample Tri6a that contains pyroxenite veins (layers) is marked by an x; cpx from the veins have the highest Al_2O_3 and Na_2O contents. In (a), plagioclase-free and plagioclase-bearing peridotites form separate trends with transitional samples straddling the two trends. Chromitites as well as fertile spinel lherzolites were collected in Duboštica. In (b) only spinel peridotites from orogenic massifs with subcontinental affinity have Na_2O contents exceeding that of DMM [87]. Relatively fertile abyssal peridotites have Na_2O contents near or below DMM. Data sources: eastern-central Alpine massifs (upper/lower Platta, UP/LP; Malenco, Mal; Totalp, Tot), Müntener et al. (2010); continental xenoliths, Witt-Eickschen and O'Neill (2005); spinel peridotites from the Gakkel ridge, Hellebrand et al. (2005); from the Southwest Indian Ridge, Seyler et al. (2003); Mirdita, Morishita et al. (2011); Lherz, Le Roux et al. (2007); Ronda, Obata (1980). (For interpretation of the references to color in this figure legend, the reader is referred to the web version of this article.)

As explained in more detail below, microstructural as well as compositional features of the plagioclase peridotites indicate that they originated by melt impregnation, rather than by subsolidus equilibration or in situ melting.

Spinel compositions from spinel peridotites in Krivaja–Konjuh cluster at the low Cr#, high Mg# end of the range of abyssal peridotites (Dick and Bullen, 1984; Arai, 1994) and spinel peridotites more generally (Arai et al., 2011; Barnes and Roeder, 2001). In contrast, plagioclase peridotites have significantly higher Cr and lower Mg numbers, creating a gap in compositions between spinel and plagioclase peridotites (Fig. 8). Abyssal peridotites have a continuum of compositions to Cr# up to 0.6, reflecting increasing depletion due to melt extraction (e.g. Hellebrand et al., 2001). The TiO_2 content of abyssal spinel peridotites is restricted to below 0.2%, while Krivaja–Konjuh transitional and plagioclase peridotites have TiO_2 contents up to 1% at essentially constant Cr# around 0.5, due to buffering of the latter by plagioclase (Chalot-Prat et al., 2013). The gap in Cr and Mg number together with the elevated TiO_2 contents implies that the composition of the transitional and plagioclase peridotites from Krivaja–Konjuh can not be due to progressive depletion by melt extraction.

Outcrop scale plagioclase patches and accumulations such as those in Fig. 4d and thin section scale plagioclase patches (Fig. 6) correlate with high TiO_2 contents of both cpx and spinel (Figs. 7, 8). Similar combinations of plagioclase patches and high TiO_2 have been described for example from the Ligurian and Corsican peridotites (Rampone et al., 1993, 1997), Lanzo (Kaczmarek and Müntener, 2008; Piccardo et al., 2007) and abyssal peridotites (Dick, 1989; Dick and Bullen, 1984; Hellebrand et al., 2002b; Rampone et al., 1997; Seyler and Bonatti, 1997; Tartarotti et al., 2002). These authors interpret the plagioclase patches as remnants of interstitially migrating melt. Spinel mantled by plagioclase observed in some locations (e.g. Fig. 6b) is found only in conjunction with interstitial plagioclase patches, suggesting the involvement of melt to enable the reaction (Piccardo et al., 2007). We therefore conclude that the plagioclase peridotites in the Krivaja–Konjuh massif are the result of melt impregnation.

Grain-scale melt migration and plagioclase crystallization introduced chemical heterogeneity at the thin-section scale. In the areas affected by infiltrating melt Al_2O_3 in cpx and spinel is not or only partially equilibrated with plagioclase. This produced populations with high and low Al_2O_3 contents at a range of TiO_2 in cpx (the parallel trends in Fig. 7a). The Eastern Central Alpine peridotites (Müntener et al., 2010) and those from Ronda epOb80 similarly straddle these two trends.

Observations from ODP Leg 153 (MARK area, Niida, 1997; Cannat et al. ,1997) show changes in compositions on a mm scale adjacent to thin gabbro veins. While gabbro veins with a range of thicknesses do occur in the plagioclase and transitional peridotites (Fig. 4b, c), the analyses shown in Figs. 7 and 8 with high TiO_2 content in cpx and spinel do not originate near or include distinct gabbro veins, but come from samples with plagioclase patches. As described above, variations in TiO_2 contents were introduced by distributed, grain scale melt infiltration; the Cr# was buffered by originally fertile spinel and plagioclase during this process. From cross-cutting relationships we infer that the gabbroveins in Krivaja represent later episodes of melt migration. Examples are shown in Fig. 4c where relatively coarser-grained gabbro veins overprint the earlier distributed, interstitial plagioclase patches, and in Fig. 4d where a thin gabbro vein located to the left of the hammer crosses the patchy plagioclase-rich areas at an angle.

Replacement of opx by olivine and cpx (Fig. 6b, d) indicates that the infiltrating melt was opx-undersaturated. This contrasts with Lanzo where opx replaced olivine (Kaczmarek and Müntener, 2008, their Fig. 7), and opx is observed at the contact between plagioclase mantling spinel and olivine (Piccardo et al., 2007, Plate IIE). Opx saturated melts were also inferred for Othris (Dijkstra et al., 2003) and the Atlantis Massif (Suhr et al., 2008). Opx undersaturation likely indicates a deeper origin of the melt (Jacques and Green, 1980; Kelemen, 1990), or a garnet pyroxenite source (Hirschmann et al., 2003). The latter has also been invoked for Ti-rich melts, although low degrees of melting of a fertile source may be sufficient (Davis et al., 2011). Deformation in the spinel peridotite field followed by infiltration of melt with a deeper origin has also been inferred for the Ligurides (Piccardo and Vissers, 2007).

In some locations coarse spinel grains in pyroxenite veins (e.g. Fig. 4b) in the plagioclase peridotites are mantled by plagioclase. However, pyroxenite veins in the spinel peridotites do not show signs of incipient melting either at the outcrop or thin-section scale (cpx in a pyroxenite vein analyzed in sample Tri6a is the most fertile in the massif (Fig. 7)). Microstructural observations also suggest that the pyroxenite veins experienced the same deformation as the peridotites, in contrast to the lack of signs of deformation of plagioclase. This indicates that the pyroxenites within the massif predate melt infiltration and are not the source of the intergranular melt in the plagioclase peridotites. This

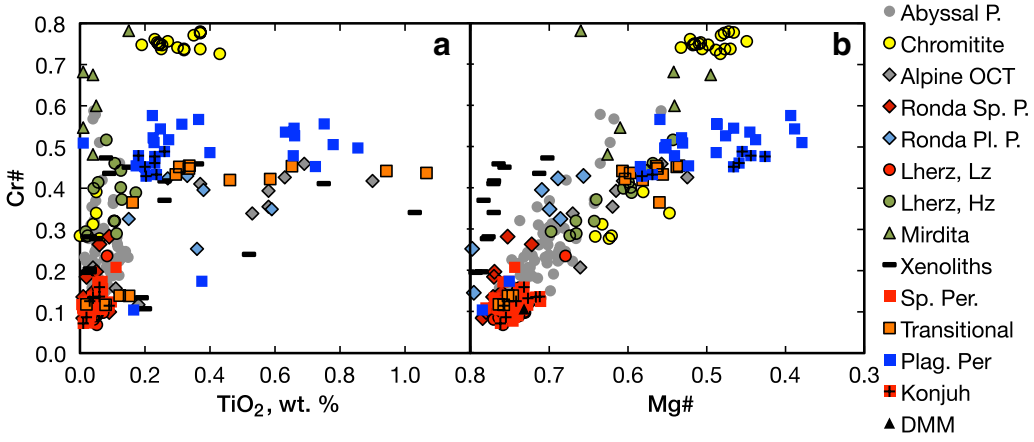

Fig. 8. Spinel compositions (a) Cr# (=Cr/Cr + Al) vs TiO_2 and (b) Cr# vs Mg# (=Mg/Mg + Fe^{2+}). For samples termed transitional relatively depleted (Cr# of 0.4 and above) large darker brown spinels and fine-grained light brown spinels (Cr# 0.1–0.2) occur in close proximity in the same thin section, similar to cpx Al_2O_3 variability. In (a) a similarly broad range in TiO_2 contents at fixed Cr# in harzburgites and dunites from the Hess Deep have been interpreted to indicate migrating melt (Dick and Bullen, 1984; Kelemen et al., 1997). The refertilized lherzolites from Lherz do not show elevated TiO_2 contents, in contrast to the plagioclase peridotites from Ronda. Spinels from massifs with supra-subduction affinity (Mirdita) and the chromitites have similar high Cr#. In (b) the data form a continuous trend, with plagioclase peridotites from KK having the highest spinel Fe contents. Noticeably off this trend are the xenoliths with higher Mg# for a given Cr#, as well as the chromitites and rocks with supra-subduction affinity. Data sources as for Fig. 7. (For interpretation of the references to color in this figure legend, the reader is referred to the web version of this article.)

is also consistent with the inference that the massif did not experience uniform heating as a whole, as the pyroxenites are expected to melt at a somewhat lower temperature relative to the peridotites (Hirschmann et al., 2003).

Among the most fertile rocks from the Krivaja–Konjuh massif are the spinel peridotites in the south and west of Krivaja that show no signs of recrystallization or high TiO_2 contents associated with melt impregnation. This contrasts with Lanzo, Ronda and Lherz, where the infiltrating melt refertilized the host rock (see e.g. the cpx Al_2O_3 contents for Lherz in Fig. 7). This process of refertilization, accompanied by textural changes and grain growth, is described as 'asthenospherisation' (e.g.Le Roux et al., 2008; Soustelle et al., 2009; Van der Wal and Vissers, 1996). In Krivaja–Konjuh the infiltrating melt enabled grain growth and precipitation of plagioclase, but led to significant compositional changes only where relatively high volumes of melt were involved, producing olivine-rich troctolites.

Evidence for continued melting at depth after the onset of rifting are more evolved melt compositions that range from olivine gabbros to gabbros, intruding into peridotite, forming large dikes or more massive outcrops. Further analysis of these rocks is needed to examine whether they are related to the melt that infiltrated the peridotites by porous flow. Late-stage, more evolved, relatively thin gabbro veins frequently cross-cut earlier dikes and veins. These later cross-cutting veins have sharp contact (Fig. 4), implying cooling of the peridotites from conditions when the earliest gabbro veins were formed. The peridotites therefore resided over a region of melt production at depth for some time.

5.3. Peridotite temperature estimates

Porphyroclastic opx grains are not obviously zoned but are compositionally heterogeneous due to exsolution lamellae, recrystallization (Fig. 5a, c) and patchy replacement by olivine and cpx (Fig. 6b, d). Due to their large size they typically are not equilibrated with smaller (recrystallized) cpx grains, which themselves can have a range of compositions in one thin section. Two-pyroxene thermometry is therefore not useful for estimating temperatures. Temperatures calculated from average opx compositions for each area with the Ca-in-opx thermometer of (Brey and Köhler, 1990) are highest for plagioclase peridotites showing evidence of melt migration (up to 1200 °C), and lowest for spinel peridotites (~900 °C) that show no sign of recovery from deformation (Table 1). Similar temperatures for plagioclase and spinel peridotites are also obtained for Lanzo, where the plagioclase peridotites are also inferred to originate by melt infiltration (Kaczmarek and Müntener, 2008).

5.4. Deformation

Highly deformed spinel lherzolites occur in the southern parts of Krivaja (Duboštica, Voj8, Fig. 5a, b); similarly deformed plagioclase lherzolites occur just to the north of the troctolites (Saj5). Rift-related deformation of the spinel lherzolites resulted in grain size reduction to mylonites and locally ultramylonites, where no porphyroclastic phase remains. With the piezometer for dry olivine of Van der Wal et al. (1993), the smallest recrystallized grain sizes of 0.1 to 0.3 mm imply stresses >20 MPa. This is significantly higher than stresses inferred for asthenospheric upper mantle of between 0.1 and 1 MPa (e.g. Behn et al., 2009), but much lower than stress estimates for low temperature ultramylonitic shear zones for example at oceanic fracture zones (Warren and Hirth, 2006) or in Oman (Linckens et al., 2011).

The lack of recovery of the spinel lherzolites implies temperatures well below the solidus during uplift and exhumation, consistent with temperature estimates from opx thermometry (Table 1). Exhumation rates on detachment faults along the Mid-Atlantic Ridge are observed to be of order of the full spreading rate of 3 cm/year (Grimes et al., 2008). Assuming a rate of 1 cm/year for the Krivaja–Konjuh massif, exhumation from within the garnet stability field would take of order of 10 Ma. With the grain growth rates for dry, melt-free olivine determined by Faul and Jackson (2007), at a temperature of 950 °C grains would grow to less than 250 μm in size during that time. Actual growth would be less since growth rates would decrease with temperature decreasing during uplift. This indicates that mylonitic grain sizes can be maintained during exhumation from significant depth, provided that temperatures remain relatively low.

The transitional and plagioclase peridotites associated with melt infiltration are characterized by recovery and grain growth. This is due to the higher temperatures indicated by opx thermometry (Table 1), as well as enhancement of grain growth due to the presence of melt (Faul and Scott, 2006). Grain growth overprints the earlier deformation evident in the spinel peridotites but does not completely erase it. Evidence for prior deformation includes dismembered and elongate olivine grains in plagioclase peridotites that are similar to those found in spinel peridotites (compare Figs. 5d and 6b), supported by the similarity of compositions in the transitional and spinel peridotites (Figs. 7, 8). In the most uniformly coarse-grained dunites and olivine-rich troctolites prior deformation is more difficult to ascertain at the thin section scale due to grain growth facilitated by higher infiltrated melt contents.

Importantly, the microstructural features due to melt infiltration in the peridotites, such as plagioclase patches and spinel grains mantled by plagioclase, as well as the microstructures of the olivine-rich troctolites as a whole, show no signs of deformation. Similarly, while some massive gabbros show evidence for deformation, thin gabbro veins in peridotites appear undeformed (Fig. 4). This implies that deformation of the peridotites essentially ceased with melt infiltration, and that processes following melt infiltration, like obduction onto the metamorphic sole during closing of the ocean basin and subsequent emplacement, did not pervasively deform the massif as a whole.

5.5. Pressure of origin

A significant feature of the clinopyroxene compositions is that the fertile spinel peridotites from Krivaja have Na_2O contents approaching primitive upper mantle values (McDonough and Sun, 1995). The high cpx Na_2O contents are similar to other orogenic peridotites such as Ronda (Obata, 1980), Beni Bousera (Gysi et al., 2011), Lherz (Le Roux et al., 2007), and the Eastern Central Alpine peridotites (Müntener et al., 2010). High Na_2O contents have been described as characteristic for subcontinental peridotites (Kornprobst et al., 1981; Seyler and Bonatti, 1994; see also Bazylev et al., 2009), but the lower Na_2O contents in abyssal peridotites were ascribed to greater depletion of the latter or metasomatic enrichment of the former.

Counter to the depletion argument is the observation that Al_2O_3 contents of cpx in fertile abyssal and orogenic peridotites are essentially the same, but the Na_2O contents in orogenic peridotites are up to twice that of abyssal peridotites (Fig. 7b). The cpx compositions of harzburgites from Lherz underscore that the difference in Na_2O between abyssal and orogenic peridotites is not primarily a function of depletion: distal harzburgites not affected by the infiltrating melt that produced the lherzolites (Le Roux et al., 2007; personal communication, 2014) have cpx Na_2O contents similar to the most fertile abyssal spinel lherzolites (up to 1%). Harzburgites close to the refertilized lherzolites and the lherzolites themselves contain twice this amount due to diffusive refertilization by Na_2O ahead of the main front. Similarly, high Na_2O contents in cpx from the Lena Trough were ascribed to a high-pressure, sub-continental origin of these rocks (Hellebrand and Snow, 2003).

The pressure dependence of clinopyroxene Na_2O contents has also been investigated experimentally. The experiments show that the Na_2O contents increase with increasing pressure. At fixed starting composition Na_2O increases from below ~1 wt.% at 1–1.5 GPa to 2 wt.% at 3 GPa, before leveling off with further pressure increase (Putirka et al., 1996; Tuff et al., 2005, see also Blundy et al., 1995). The experimental

observations suggest therefore that the high Na_2O contents of the orogenic peridotites are due to their higher pressure origin relative to abyssal peridotites. A high pressure origin for the orogenic peridotites is supported by the occurrence of garnet pyroxenites in these massifs. Additionally, modeling by Müntener et al. (2010) shows that Na-rich but Nd-poor cpx compositions of the Alpine peridotites indicate melting in the garnet stability field.

Independent indications of a relatively high pressure origin of the spinel peridotites from Krivaja come from microstructural observations. While no garnet has yet been observed in the pyroxenites, garnet-shaped symplectites (Fig. 5f) and coarse opx-spinel symplectites in peridotites (Fig. 5e) occur in a number of locations (Tajašnica, Duboštica, Sajavica). The orthopyroxene in the symplectite in Fig. 5e shows exsolution lamellae, like other opx porphyroclasts. In Lanzo and Mt. Maggiore (Corsica) finer scale symplectites, consisting of spinel plus opx without exsolution lamellae, occur within opx porphyroclasts near their grain boundaries. The latter are interpreted as being due to exsolution of Al from opx during cooling (Piccardo et al., 2007; Rampone et al., 2008). The coarse symplectites, representing individual grains, are interpreted as originating from breakdown of garnet at spinel-facies conditions.

From the combination of microstructural observations and Na_2O-rich cpx we infer a relatively high pressure, subcontinental origin for the spinel peridotites found in the Krivaja. Na_2O contents below DMM for the fertile spinel peridotites from Konjuh with similar cpx Al_2O_3 contents indicate a lower pressure origin, similar to fertile abyssal peridotites.

5.6. Traces of subduction

The compositions of the chromitites near Duboštica (see Fig. 2 and Table 1) are distinct from all other compositions found in the massif (Figs. 7, 8). Their Cr# are similar to harzburgites and dunites from the Eastern Mirdita ophiolite, which has supra-subduction affinity (Dilek, 2003; Dilek et al., 2005; Morishita et al., 2011), but the Krivaja chromitites have somewhat higher Mg# and TiO_2 contents. Compositions in the Krivaja–Konjuh massif are too fertile to produce melts that would be in equilibrium with the Cr# found in the chromitites (Arai, 1994; Arai et al., 2011). Barnes and Roeder (2001) note that boninites are the only group of magmas that commonly contain spinels that are as Cr-rich as those typical of ophiolitic chromitites. Due to the low solubility of Cr-spinel in silicate melts chromitites require melt-rock ratios of more than 300 to form (Kelemen et al., 1997). The absence of significant outcrops of dunite in the Krivaja, with which chromitites are usually associated, also indicates that the melt that produced the chromitites is not derived from the massif itself.

Since the chromitites appear to be unrelated to the massif we infer that they represent a later episode of melt migration. The metamorphic sole indicates that the massif was thrust onto oceanic crust, prior to obduction and inclusion in the mélange. The composition of the chromitites suggests a subduction-related origin, indicating that the massif was the upper plate during closure of the ocean basin. Depleted and hydrous melts from the mantle wedge below traversed the Krivaja peridotites in localized conduits. Their fertile compositions imparted a higher spinel Mg# and cpx TiO_2 content in comparison to most chromitites (Barnes and Roeder, 2001), although temperature can also affect spinel Mg# (Arai et al., 2011). These localized melt conduits may be related to basaltic dikes in the south-eastern part of the massif that have suprasubduction major and trace element affinity (Lugović et al., 2006). The important implication is that particularly in the western Dinarides volcanics with supra-subduction affinity are unlikely to be related to the peridotites that have fertile, subcontinental characteristics.

5.7. Summary of the compositional characteristics of Krivaja and Konjuh

Comparison of the compositions of the two parts of the massif with each other and with peridotites from different tectonic settings places constraints on the likely origin of rocks from the massif. As discussed above, the high cpx Na_2O contents indicate a subcontinental origin of parts of Krivaja. In contrast, the spinel peridotites in Konjuh have significantly lower cpx Na_2O contents. Comparison with cpx compositions from spinel peridotites from the Gakkel ridge, described as covering the range of global compositions (Hellebrand et al., 2005), and those from the Southwest Indian Ridge, tending towards more enriched compositions (Seyler et al., 2003), shows that they have Al_2O_3 contents as high to those from Krivaja–Konjuh and other orogenic peridotites. However, their TiO_2 contents are restricted to below 0.4 wt.%, similar to peridotites from Konjuh and a massif inferred to represent oceanic lithosphere (Monte del Estados, Puerto Rico, Marchesi et al., 2011). Spinel peridotites from orogenic massifs such as Lherz (Le Roux et al., 2007), Ronda (Obata, 1980) and the Alps (Müntener et al., 2010) overlap the compositional range of TiO_2 and Al_2O_3 in cpx of Krivaja, but only the Alpine plagioclase peridotites extend to similarly high TiO_2 contents. Spinel TiO_2 contents in Konjuh are also lower than Krivaja.

Spinel peridotites from Krivaja–Konjuh do not range to the depleted end of abyssal harzburgites with cpx Al_2O_3 contents as low as 2% and TiO_2 contents below 0.1% (e.g. from the Mid-Atlantic Ridge, Seyler et al., 2007, Hess Deep, Arai and Matsukage, 1996, Fig. 7). The depleted abyssal peridotite compositions overlap with the Eastern Mirdita ophiolite which is inferred to originate in a supra-subduction setting (Dilek, 2003; Morishita et al., 2011).

The significance of the shear zone between the Krivaja and Konjuh portions is not obvious, as some of the more depleted south-eastern parts of Krivaja (Vojnica and Tribija) are also lacking the TiO_2 and Na_2O enrichment, similar to Konjuh. Other indicators of fertility such as cpx Al_2O_3 contents, olivine Mg# and spinel Cr# and Mg# cover the same range in both parts. Konjuh also appears not to have experienced the same high degree of deformation as the fertile spinel peridotites from Krivaja. The latter locally have no porphyroclasts remaining, but the fertile spinel peridotites from Konjuh show only partial recrystallization of olivine, with pyroxene affected by deformation but not recrystallized. Overall the compositional characteristics of Krivaja indicate a subcontinental origin, while those of Konjuh suggest an suboceanic origin. However, both parts are similar in their fertility.

6. Relationship to the Balkan peridotite massifs

For the tectonic context it is useful to clarify the names of the respective units found in the literature. The Dinaride Ophiolite belt and Vardar Zone Western Belt as described here (Bazylev et al., 2009; Karamata, 2006; Pamić et al., 2002) are collectively referred to as the Western Vardar Ophiolitic Unit by Schmid et al. (2008) to distinguish it from the ophiolites of the Eastern Vardar Ophiolitic Unit (or Main Vardar Belt, Karamata, 2006), separated from the Western Unit by the Sava Zone. The following refers only to the Western Vardar Ophiolitic Unit (i.e. Dinarides and Vardar Zone Western Belt).

Differences in the petrology and geochemistry between the Dinaride and Vardar zone belts (e.g. Lugović et al., 1991) have been used to infer that the two belts originated in different ocean basins (e.g. Dilek et al., 2008; Karamata, 2006; Pamić et al., 2002; Robertson and Karamata, 1994 and references therein). In contrast, some authors have invoked a single ocean model for the origin of both belts (e.g. Schmid et al., 2008; Smith and Spray, 1984). In light of these different models we compare compositions from the Krivaja–Konjuh massif from this study to compositions from other peridotite massifs from both the Dinarides and the Vardar zone (Bazylev et al., 2009), as well as the Mirdita ophiolite in Albania from Morishita et al. (2011).

Whole rock analyses were performed by Lugović et al. (1991) for Krivaja–Konjuh and by Bazylev et al. (2009) for a number of massifs within the Dinarides and Vardar zone. Fig. 9 shows anhydrous whole rock compositions for the oxides Al_2O_3 and TiO_2, considered least affected by alteration. The compositions of the Krivaja–Konjuh spinel lherzolites (Lugović et al., 1991) and the western massifs of the Dinarides (Bazylev et al., 2009) (see Fig. 1) are comparable to the

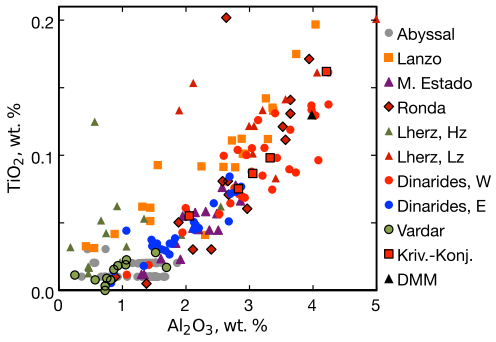

Fig. 9. Select anhydrous whole rock compositions from orogenic massifs (Bodinier et al., 1988; Frey et al., 1985; Le Roux et al., 2007), an oceanic massif (Monte del Estado, Marchesi et al., 2011) and abyssal peridotites (Casey, 1997) compared to compositions from the Krivaja–Konjuh massif itepLu91 and the Dinarides and Vardar Zone (Bazylev et al., 2009). DMM from Workman and Hart (2005). The compositions from the western Dinarides overlap with orogenic massifs, while the eastern Dinarides are more similar to compositions from a relatively fertile oceanic massif.

relatively fertile compositions of other orogenic massifs such as Lherz (Le Roux et al., 2007), Ronda (Frey et al., 1985) and Lanzo (Bodinier et al., 1988). The eastern massifs of the Dinarides are somewhat less fertile, comparable to compositions from the Monte del Estado massif, described as originating from oceanic lithosphere (Marchesi et al., 2011). At the more depleted end rocks from the Vardar zone are similar to depleted abyssal peridotites (Casey, 1997).

Clinopyroxene Na_2O vs Al_2O_3 separates different groups of massifs (Fig. 10a). To exclude the effects of plagioclase crystallization on clinopyroxene compositions only spinel peridotites are plotted. Fig. 10 shows that compositions from Krivaja–Konjuh cover the same range as the western massifs of the Dinaride ophiolite belt (Borja, Ljubić–Čavka, Bistrica, Sjenički Ozren; see Fig. 1). The effect of pressure on cpx Na_2O content is emphasized by the fact that Al_2O_3 only decreases moderately for a range of Na_2O from 2 to 1 wt.%, with fertile rocks from Konjuh at the low end of the range. The massifs on the eastern side of the Dinarides (Bosanski Ozren, Zlatiborand Banjska), show decreasing Al_2O_3 contents at Na_2O below 1 wt.%. The Banjska massif is usually considered part of the Vardar zone, but due to its fertility (cpx $Al_2O_3 > 4$ wt.%, bulk rock > 1.6 wt.%) it is grouped here with the eastern massifs of the Dinarides, rather than the Vardar zone (cpx $Al_2O_3 < 3$ wt.%, bulk rock $< 1\%$). Below 0.25 wt.% Na_2O the Al_2O_3 content drops quickly, but rocks from the Vardar Zone still have consistently higher values compared to Mirdita, Tuzinje and Brezovica.

The same groups are also identifiable in the spinel compositions (Fig. 10b). The Dinarides include compositions that coincide with the fertile end of abyssal peridotites (Fig. 8), (e.g. Dick and Bullen, 1984), while rocks from the Vardar zone range to compositions that overlap with arc harzburgites (Arai, 1994; Ishii et al., 1992). The plagioclase peridotites from Krivaja–Konjuh and the western massifs of the Dinarides diverge from the depletion trend to elevated TiO_2 contents. The western massifs therefore are characterized by melt infiltration, possibly at the onset of rifting, while the eastern massifs and the Vardar zone either show only the effects of depletion, or migrating melts were of a different character, not enriched in TiO_2.

Overall the clinopyroxene compositions of the Balkan peridotite massifs show a decrease in Na_2O from west to east, indicating decreasing pressures of equilibration. Fertility also decreases systematically as shown by mineral and bulk rock compositions (Figs. 9 and 10). This suggests a gradual progression in tectonic setting from subcontinental on the western edge of the Dinarides, to fertile abyssal peridotite compositions of Konjuh to somewhat more depleted compositions of the eastern massifs. Compositions of the Vardar Zone massifs are at the depleted end of abyssal peridotites, possibly transitioning to supra-subduction affinity. Grouping the Banjska massif with the eastern Dinarides due to their similar fertility forms a continuous structural trend of parallel bands from south of the Alps to the Hellenides (Fig. 1). The gradual change in compositions from west to east is consistent with the 'single ocean' hypothesis of the peridotite massifs of the Dinarides and Vardar zone of Schmid et al. (2008) with a fertile western continental margin and a depleted, possibly subduction influenced margin on the eastern side.

In contrast to the gradual change from west to east, there is a distinct break in compositions at the southern end of the Dinarides. While Sjenički Ozren shows subcontinental affinity, the Eastern Mirdita and Brezovica massifs have been linked to a supra-subduction setting (Bazylev et al., 2003; Dilek et al., 2008; Morishita et al., 2011). A distinct drop in fertility occurs over a distance of only about 20 km between Sjenički Ozren with Al_2O_3 between 4–7% and the Tuzinje massif with

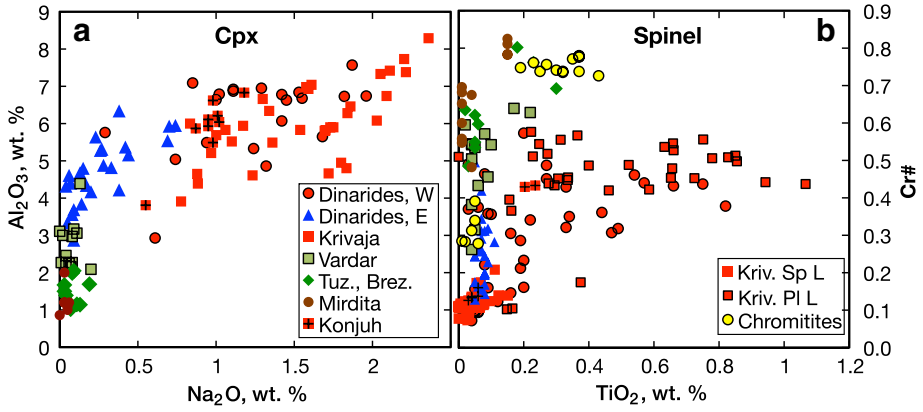

Fig. 10. Peridotite compositions from Krivaja–Konjuh (this study, Šegvić, 2010), the Dinarides and Vardar zone (Bazylev et al., 2009), as well as the Mirdita ophiolite in Albania (Morishita et al., 2011). Symbol colors correspond to colors in Fig. 1. (a) Cpx Al_2O_3 vs Na_2O for spinel peridotites only. Data from the pyroxenite in Tri6a are not shown. Overall the data form a continuous trend with Al_2O_3 contents only deceasing substantially below 0.5 wt.% Na_2O. The western Dinarides are the most fertile, while the massifs on the eastern side (Zlatibor and Bosanski Ozren) are more depleted, overlapping with Vardar zone compositions. Compositions from Brezovica and Tuzinje in the south overlap with the Eastern Mirdita ophiolite with supra-subduction affinity (Dilek, 2003; Dilek et al., 2008; Morishita et al., 2011). (b) Spinel Cr# vs TiO_2 content. As for clinopyroxene the spinel compositions show progressive depletion from west to east. The plagioclase peridotites deviate from this trend at Cr# between 0.4 and 0.6 due to the effects of melt migration (see text). The Brezovica and Tuzinje spinels have the highest Cr#, along with the chromitites from the southern part of Krivaja, similar to compositions from Eastern Mirdita. (For interpretation of the references to color in this figure legend, the reader is referred to the web version of this article.)

less than 2%. A similar contrast in fertility exists between the Banjska massif and the massifs to the south.

The Peć-Srbica line (or Scutari-Peć lineament) is inferred to represent a structural break between the Dinarides and Hellenides (e.g. Smith, 1993) and has been interpreted as a transform fault between a rift basin to the northwest and a small ocean basin to the southeast (Robertson et al., 2009). Dilek et al., (2005), citing the complete ophiolitic sequence of the Western Mirdita massif with extensive volcanics just to the south of the line, argue that this productivity is incompatible with a fracture zone, and that it belonged to a spreading center. A further complication is that the Tuzinje massif is compositionally more similar to the depleted massifs to the south (Bazylev et al., 2009), but lies to the north of this line.

7. Evolution of the Krivaja–Konjuh Massif

The structural and petrological observations detailed above can be placed in the context of the tectonic evolution of the Balkans discussed in a range of publications. A number of the observations and inferences need to be further substantiated, the following is intended to provide a framework for this. The ophiolites of the Dinarides and Vardar zone are inferred to be at least of early Triassic age, originating in a Tethys-associated ocean (e.g. Pamić et al., 2002). Rift related igneous and sedimentary rocks are of late Permian age, while radiolarian cherts associated with MOR type basalts are dated as late Triassic (Robertson et al., 2009). Agreed upon dates exist only for the metamorphic sole of the Krivaja–Konjuh massif, with ages ranging from 174–157 Myr. As described below, the peridotites record earlier processes related to the opening of the ocean basin.

The earliest record in the massif is the deformation of the spinel lherzolites (Fig. 11a). Significant strain is indicated by the degree of recrystallization, locally to ultramylonites. Based on the calculated temperature, lack of recovery and high cpx Na_2O contents of these rocks the deformation took place at relatively high pressures and lithospheric temperatures, representing lithospheric thinning at the onset of rifting. Continued thinning of the lithosphere resulted in upwelling of asthenosphere and onset of melting at depth, producing opx-undersaturated melts. On upward migration this melt infiltrated portions of the thinned lithosphere, heating it (Fig. 11b). This resulted in partial conversion of spinel to plagioclase and the onset of recovery and grain growth seen in the transitional and plagioclase peridotites. Melt impregnation overprinted but did not erase the texture originating with lithospheric extension.

The fault structures in the massif suggest exhumation of the peridotites along localized shear zones without further pervasive deformation (Fig. 11c). The relatively low volumes of melt produced at depth froze in the thermal boundary layer either as interstitial melt in plagioclase peridotites, troctolites or gabbro intrusions. This lead to exposure of peridotites at the seafloor without volcanic cover, producing ophicalcites.

Progressive thinning resulted in melting to shallower depth with overall higher melt production and consequent greater depletion of the peridotites, recorded in the eastern Dinarides (Fig. 11d). Continued spreading then migrated eastwards towards the Vardar zone. In this scenario the Krivaja would represent the western margin of the

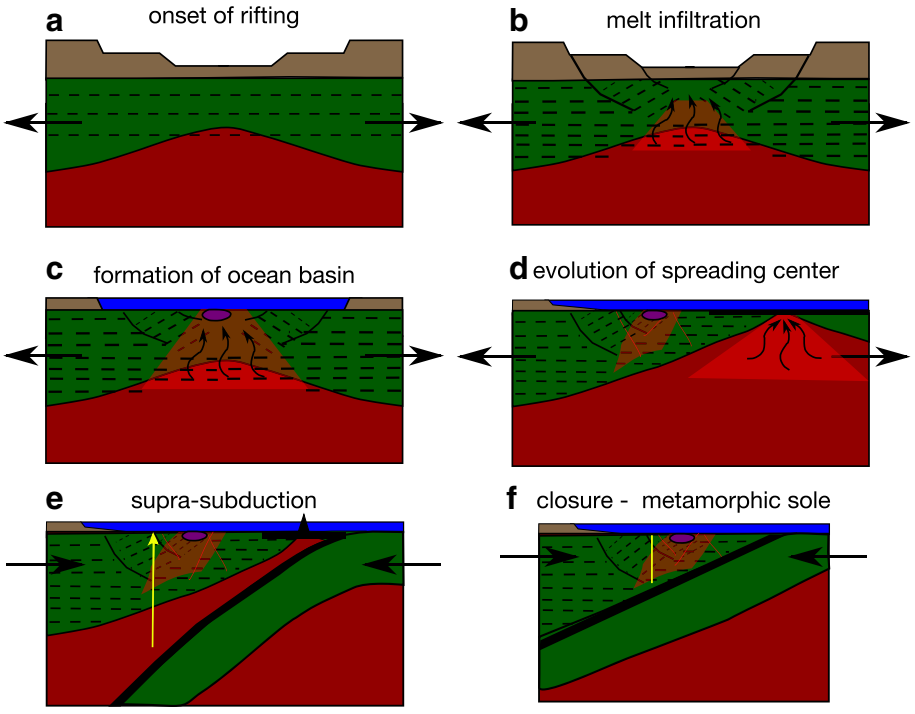

Fig. 11. Evolution of the Krivaja–Konjuh massif and the Dinarides and Vardar zone. The model follows those proposed for example by Pamić et al. (2002) and Robertson et al. (2009), but accounts for specific events identifiable in the peridotites of the Krivaja–Konjuh massif. (a) Onset of lithospheric thinning. Pervasive deformation, at lithospheric temperatures and pressures near the spinel garnet transition. Possible onset of localization. (b) Onset of melting in upwelling asthenosphere and infiltration of the melt into the thinned lithosphere. Melt infiltration raises the temperature, enabling reaction to plagioclase and recrystallization. Melt impregnation overprints but does not erase pre-existing texture. Deformation further localizes in shear zones. (c) Creation of an ocean basin due to continued extension. Exhumation of peridotites to the ocean floor. Continued melting and migration of deeper melt converts some plagioclase peridotites to troctolites. Intrusion of massive gabbros accommodates extension without further pervasive deformation. (d) Evolution of the spreading center to a mid-ocean ridge. Melting to shallower depth leads to increasing depletion of peridotites, forming the Eastern Dinarides and possibly Vardar zone peridotites. (e) Subduction and beginning of closure of the ocean basin. Dinarides are part of the overriding plate locally traversed by mantle-wedge derived melts, forming the chromitites and other supra-subduction related volcanics in the Krivaja–Konjuh massif and Dinarides. Vardar zone may be a backarc spreading center. (f) Closure of the ocean basin pushes Dinarides onto subducting slab, creating the metamorphic sole. Continued shortening leads to obduction and incorporation into the melange.

Meliata–Maliac Ocean, separated from the Neotethys to the east by a spreading ridge in the Late Triassic (Schmid et al., 2008).

The next distinct record is the chromitites in the south of Krivaja, interpreted as localized conduits for subduction related melts. This implies that the Krivaja was the overriding plate above a subducting slab (Fig. 11e). Progressive subduction formed the approximately west–east aligned series of chromitites (Federal Geological Institute, 1971–1990), as well as other supra-subduction-related volcanics, which are not considered to be co-magmatic with the peridotites (Bazylev et al., 2009). Depleted rocks such as harzburgites and dunites in otherwise relatively fertile massifs of the Dinarides may similarly represent localized suprasubduction-related melt migration. This is suggested by the flat or spoon-shaped cpx trace element patterns of harzburgites and dunites from Bistrica and Zlatibor that contrast with the more LREE depleted, but significantly higher M-HREE patterns of the lherzolites from these massifs (Bazylev et al., 2009). While the latter are interpreted to reflect low degrees of partial melting, the former are associated with chromatographic effects or advective melt transport (Hellebrand et al., 2002a). By comparison, cpx from the suprasubduction-related Brezovica massif have U-shaped patterns with significantly enriched LREE.

Intra-oceanic subduction closed the ocean basin during the Jurassic, generating the metamorphic sole (Fig. 11f). On closure of the ocean basin, the massif, including the metamorphic sole, was obducted onto the Adriatic plate and thrust onto the Triassic and Jurassic limestones in the ophiolitic mélange. Diapiric emplacement of the massif as a whole in its current position within the mélange is precluded by the low temperature conditions during emplacement indicated by the contact of peridotite with the underlying limestone. As indicated above, the southern end of the Dinarides at the transition to the Albanian ophiolites has a different, supra-subduction related character, indicating a somewhat different origin.

8. Conclusions

The peridotites of the Krivaja–Konjuh massif record a complex history that ranges from early rifting to traces of subduction. In the Krivaja fertile peridotites of relatively high pressure origin are pervasively deformed at lithospheric temperatures, likely recording rifting of subcontinental lithosphere. Some of these rocks are subsequently infiltrated by a melt of deeper origin, causing changes in the mineral modes and assemblage (dissolution of opx and precipitation of plagioclase), as well as recovery and grain growth. The rocks affected by melt infiltration show no further deformation. The most fertile portions of Konjuh are similar in composition to the fertile portions of Krivaja, but do not show the high pressure signature and are not as highly deformed. Plagioclase peridotites have the same textural characteristics indicating melt infiltration as in Krivaja, but are not as enriched in TiO_2. Harzburgites and dunites are essentially absent, but large areas of olivine-rich troctolites occur in the center of Krivaja.

In the southern part of Krivaja very localized migration of a much more depleted melt with possible boninitic affinity is recorded by the occurrence of chromitites. The compositions of spinels in the chromitites are distinctly different and have no counterpart anywhere else within the massif, either in ultramafic or mafic lithologies. The chromitites, however, maybe linked to the volcanic rocks with supra-subduction affinity found in the vicinity of the massif. This suggests that the chromitites were created during closing of the ocean basin, where the Krivaja–Konjuh massif was the upper plate of a subduction system.

The range of compositions found in the Krivaja–Konjuh massif is similar to the range observed for the western massifs of the Dinaride ophiolite belt. The trend of decreasing fertility, from subcontinental affinity in the western part of the Dinarides to depleted compositions in the Vardar zone (Fig. 1) corresponds to an ocean–continent transition as envisioned for remnants of the Alpine Tethys. In contrast, the transition to the Albanian and Greek ophiolites, which are much more depleted relative to the Dinarides and are associated with a supra-subduction setting, appears to be localized rather than gradual.

Acknowledgements

Reviews of an earlier version by Carlos Garrido and Shoji Arai and by two anonymous reviewers improved the manuscript. The help of Neel Chatterjee and Bob Rapp with microprobe analyses is gratefully acknowledged. This work was partially supported by NSF grant EAR 0838447 to UF.

Appendix A. Supplementary data

Supplementary data to this article can be found online at http://dx.doi.org/10.1016/j.lithos.2014.05.026.

References

Arai, S., 1994. Characterization of spinel peridotites by olivine–spinel compositional relationships: review and interpretation. Chemical Geology 113, 191–204.
Arai, S., Matsukage, K., 1996. Petrology of the gabbro–troctolite–peridotite complex, Hess Deep, equatorial Pacific: implications for mantle–melt interactions within the oceanic lithosphere. In: Mével, C., Gillis, K.M., Allan, J.F., Meyer, P.S. (Eds.), Proc. Ocean Drill. Program, Scientific Results, Vol. 147. ODP, College Station, Tx, pp. 135–155.
Arai, S., Okamura, H., Kadoshima, K., Tanaka, C., Suzuki, K., Ishimaru, S., 2011. Chemical characteristics of chromian spinel in plutonic rocks: implications for deep magma processes and discrimination of tectonic setting. Island Arc 20, 125–137.
Armstrong, J.T., 1995. CITZAF—a package for correction programs for the quantitative electron microbeam X-ray analysis of thick polished materials, thin-films and particles. Microbeam Analysis 4, 177–200.
Barnes, S.J., Roeder, P.L., 2001. The range in spinel compositions in terrestrial mafic and ultramafic rocks. Journal of Petrology 42, 2279–2302.
Bazylev, B.A., Karamata, S., Zakariadze, G.S., 2003. Petrology and evolution of the Brezovica ultramafic massif, Serbia. Geological Society, London, Special Publications 218, 91–108. http://dx.doi.org/10.1144/GSL.SP.2003.218.01.06 (91-108).
Bazylev, B.A., Popević, A., Karamata, S., Kononkova, N., Simakin, S., Olujić, J., Vujnović, L., Memović, E., 2009. Mantle peridotites from the Dinaridic ophiolite belt and the Vardar zone western belt, central Balkan: a petrological comparison. Lithos 108, 37–71. http://dx.doi.org/10.1016/j.lithos.2008.09.011.
Behn, M.D., Hirth II, G., J. R. E., 2009. Implications of grain size evolution on the seismic structure of the oceanic upper mantle. Earth and Planetary Science Letters 282, 178–189. http://dx.doi.org/10.1016/j.epsl.2009.03.014.
Blundy, J.D., Falloon, T.J., Wood, B.J., Dalton, J.A., 1995. Sodium partitioning between clinopyroxene and silicate melts. Journal of Geophysical Research 100, 15,501–15,515.
Bodinier, J.-L., Dupuy, C., Dostal, J., 1988. Geochemistry and petrogenesis of Eastern Pyrenean peridotites. Geochimica et Cosmochimica Acta 52, 2893–2907.
Brey, G.P., Köhler, T., 1990. Geothermobarometry in four-phase lherzolites II. New thermobarometers, and practical assessment of existing thermobarometers. Journal of Petrology 31, 1353–1378.
Cannat, M., 1993. Emplacement of mantle rocks in the sea-floor at mid-ocean ridges. Journal of Geophysical Research 98, 4163–4172.
Cannat, M., Chatin, F., Whitechurch, H., Ceuleneer, G., 1997. Gabbroic rocks trapped in the upper mantle at the Mid-Atlantic Ridge. In: Karson, J.A., Cannat, M., Miller, D.J., Elton, D. (Eds.), Proceedings of the Ocean Drilling Program, Scientific Results, vol. 153. Ocean Drilling Program, College Station, TX, pp. 243–264.
Casey, J.F., 1997. Comparison of major and trace-element geochemistry of abyssal peridotites and mafic plutonics with basalts from the MARK region of the Mid-Atlantic ridge. In: Karson, J.A., Cannat, M., Miller, D.J., Elton, D. (Eds.), Proceedings of the Ocean Drilling Program, Scientific Results, vol. 153. Ocean Drilling Program, College Station, TX, pp. 181–241.
Chalot-Prat, F., Falloon, T.J., Green, D.H., Hibberson, W.O., 2013. Melting of plagioclase + spinel lherzolite at low pressures (0.5 GPa): an experimental approach to the evolution of basaltic melt during mantle refertilisation at shallow depths. Lithos 172–173, 61–80.
Davis, F.A., Hirschmann, M.M., Humayun, M., 2011. The composition of the incipient partial melt of garnet peridotite at 3 GPa and the origin of OIB. Earth and Planetary Science Letters 308, 380–390.
Dick, H.J.B., 1989. Abyssal peridotites, very slow spreading ridges and ocean ridge magmatism. Geological Society, London, Special Publications 42, 71–105.
Dick, H.J.B., Bullen, T., 1984. Chromian spinel as a petrogenetic indicator in abyssal and alpine-type peridotites and spatially associated lavas. Contributions to Mineralogy and Petrology 86, 54–76.
Dick, H.J.B., Lissenberg, C.J., Warren, J.M., 2010. Mantle melting, melt transport, and delivery beneath a slow-spreading ridge: the paleo-MAR from 23°15′N to 23°45′N. Journal of Petrology 51, 425–467.
Dijkstra, A.H., Barth, M.G., Mason, M.R.D.P.R.D., Vissers, R.L.M., 2003. Diffuse porous melt flow and melt-rock reaction in the mantle lithosphere at a slow-spreading ridge: a structural petrology and LA-ICP-MS study of the Othris peridotite massif (Greece). Geochemistry, Geophysics, Geosystems 4, 8613. http://dx.doi.org/10.1029/2001GC000278.

Dilek, Y., 2003. Ophiolite concept and its evolution. In: Dilek, Y., Newcomb, S. (Eds.), Ophiolite Concept and the Evolution of Geological Thought, vol. 373. Geological Society of, America, pp. 1–16 (of Special Paper).
Dilek, Y., Furnes, H., 2011. Ophiolite genesis and global tectonics: geochemical and tectonic fingerprinting of ancient oceanic lithosphere. GSA Bulletin 123, 387–411. http://dx.doi.org/10.1130/B30446.1.
Dilek, Y., Shallo, M., Furnes, H., 2005. Rift drift, seafloor spreading and subduction tectonics of Albanian ophiolites. International Geology Review 47, 147–176.
Dilek, Y., Furnes, H., Shallo, M., 2008. Geochemistry of the Jurassic Mirdita ophiolite (Albania) and the MORB to SSZ evolution of a marginal basin oceanic crust. Lithos 100, 174–209.
Faul, U.H., Jackson, I., 2007. Diffusion creep of dry, melt-free olivine. Journal of Geophysical Research 110, B04204. http://dx.doi.org/10.1029/2006JB004586.
Faul, U.H., Scott, D., 2006. Grain growth in partially molten olivine aggregates. Contributions to Mineralogy and Petrology 151, 101–111.
Federal Geological Institute, 1971–1990. Basic Geologic maps of SFRJ. Belgrade.
Frey, F.A., Suen, C.J., Stockman, H.W., 1985. The Ronda high temperature peridotite: geochemistry and petrogenesis. Geochimica et Cosmochimica Acta 49, 2469–2491.
Grimes, C.B., John, B.E., Cheadle, M.J., Wooden, J.L., 2008. Protracted construction of gabbroic crust at a slow spreading ridge: constraints from $^{206}Pb/^{238}U$ zircon ages from Atlantis Massif and IODP Hole U1309D (30°N, MAR). Geochemistry, Geophysics, Geosystems 9. http://dx.doi.org/10.1029/2008GC002063 Q08012.
Gysi, A.P., Jagoutz, O., Schmidt, M.W., Targuisti, K., 2011. Petrogenesis of pyroxenites and melt infiltrations in the ultramafic complex of Beni Bousera, northern Morocco. Journal of Petrology 52, 1679–1735.
Hellebrand, E., Snow, J.E., 2003. Deep melting and sodic metasomatism underneath the highly oblique-spreading Lena Trough (Arctic Ocean). Earth and Planetary Science Letters 216, 283–299.
Hellebrand, E., Snow, J.E., Dick, H., Hoffmann, A., 2001. Coupled major and trace elements as indicators of the extent of melting in mid-ocean-ridge peridotites. Nature 410, 677–681.
Hellebrand, E., Snow, J.E., Hoppe, P., Hofmann, A.W., 2002a. Garnet-field melting and late-stage refertilization in 'residual' abyssal peridotites from the Central Indian Ridge. Journal of Petrology 43, 2305–2338.
Hellebrand, E., Snow, J.E., Mühe, R., 2002b. Mantle melting beneath Gakkel Ridge (Arctic Ocean): abyssal peridotite spinel compositions. Chemical Geology 182, 227–235.
Hellebrand, E., Snow, J.E., Mostefaoui, S., Hoppe, P., 2005. Trace element distribution between orthopyroxene and clinopyroxene in peridotites from the Gakkel ridge: a SIMS and NanoSIMS study. Contributions to Mineralogy and Petrology 150, 486–504. http://dx.doi.org/10.1007/s00410-005-0036-5.
Hirschmann, M.M., Kogiso, T., Baker, M.B., Stolper, E.M., 2003. Alkalic magmas generated by partial melting of garnet pyroxenite. Geology 31, 481–484.
Hrvatović, H., Pamić, J., 2005. Principal thrust–nappe structures of the Dinarides. Acta Geologica Hungarica 48, 133–151.
Ishii, T., Robinson, P.T., Maekawa, H., Fiske, R., 1992. Petrological studies of peridotites from diapiric serpentinite seamounts in the Izu–Ogasawara–Mariana forearc, Leg 125. In: Fryer, P., Pearce, J.A., Stokking, L.B., et al. (Eds.), Proceedings of the Ocean Drilling Program, Scientific Results, vol. 125. Ocean Drilling Program, College Station, TX, pp. 445–486.
Jacques, A.L., Green, D.H., 1980. Anhydrous melting of peridotite at 0–15 kb pressure and the genesis of tholeiitic basaits. Contributions to Mineralogy and Petrology 73, 287–310.
Kaczmarek, M.-A., Müntener, O., 2008. Juxtaposition of melt impregnation and high-temperature shear zones in the upper mantle; field and petrological constraints from the Lanzo peridotite (northern Italy). Journal of Petrology 49, 2187–2220. http://dx.doi.org/10.1093/petrology/egn065.
Karamata, S., 2006. The geological development of the Balkan Peninsula related to the approach, collision and compression of Gondwanan and Eurasian units. Geological Society, London, Special Publications 260, 155–178.
Kelemen, P.B., 1990. Reaction between ultramafic rock and fractionating basaltic magma. I. Phase relations, the origin of calc-alkaline magma series, and the formation of discordant dunite. Journal of Petrology 31, 51–98.
Kelemen, P.B., Matter, J., 2008. In situ carbonation of peridotite for CO^2 storage. PNAS 105, 17295–17300.
Kelemen, P.B., Hirth, G., Shimizu, N., Spiegelman, M., Dick, H.J.B., 1997. A review of melt migration processes in the adiabatically upwelling mantle beneath oceanic spreading ridges. Philosophical Transactions of the Royal Society of London A 355, 283–318.
Kornprobst, J., Ohnenstetter, D., Ohnenstetter, M., 1981. Na and Cr contents in clipyroxenes from peridotites: a possible discriminant between "sub-continental" and "sub-oceanic" mantle. Earth and Planetary Science Letters 53, 241–254.
Lagabrielle, Y., Bodinier, J.L., 2008. Submarine reworking of exhumed subcontinental mantle rocks: field evidence from the Lherz peridotites, French Pyrenees. Terra Nova 20, 11–21. http://dx.doi.org/10.1111/j.1365-3121.2007.00781.x.
Le Roux, V., Bodinier, J.-L., Tommasi, A., Alard, O., Dautria, J.-M., Vauchez, A., Riches, A.J.V., 2007. The lherz spinel lherzolite: refertilized rather than pristine mantle. Earth and Planetary Science Letters 259, 599–612.
Le Roux, V., Tommasi, A., Vauchez, A., 2008. Feedback between melt percolation and deformation in an exhumed lithosphere–asthenosphere boundary. Earth and Planetary Science Letters 274, 401–413. http://dx.doi.org/10.1016/j.epsl.2008.07.053.
Linckens, J., Herwegh, M., Müntener, O., 2011. Linking temperature estimates and microstructures in deformed polymineralic mantle rocks. Geochemistry, Geophysics, Geosystems 12, Q08004. http://dx.doi.org/10.1029/2011GC003536.
Lugović, B., Altherr, R., Raczek, I., Hoffmann, A., Majer, V., 1991. Geochemistry of peridotites and mafic igneous rocks from the Central Dinaric ophiolite belt, Yugoslavia. Contributions to Mineralogy and Petrology 106, 201–216.
Lugović, B., Šegvić, B., Babajić, E., Trubelja, F., 2006. Evidence of short-living intraoceanic subduction in the Central Dinarides, Konjuh ophiolite complex (Bosnia–Herzegovina). International Sypmpsium on Mesozoic Ophiolite Belts of the Northern Part of the Balkan Peninsula, pp. 72–75 (Vol. Belgrade, Serbia).
Marchesi, C., Jolly, W.T., Lewis, J.F., Garrido, C.J., Proenza, J.A., Lidiak, E.G., 2011. Petrogenesis of fertile mantle peridotites from the Monte del Estado massif (southwest Puerto Rico): a preserved section of proto-Caribbean lithospheric mantle? Geologica Acta 9, 289–306.
McDonough, W.F., Sun, S.-S., 1995. The composition of the Earth. Chemical Geology 120, 223–253.
Morishita, T., Dilek, Y., Shallo, M., Tamura, A., Arai, S., 2011. Insight into the uppermost mantle section of a maturing arc: the eastern Mirdita ophiolite, Albania. Lithos 124, 215–226. http://dx.doi.org/10.1016/j.lithos.2010.10.003.
Müntener, O., Manatschal, G., Desmurs, L., Pettke, T., 2010. Plagioclase peridotites in ocean–continent transitions: refertilized mantle domains generated by melt stagnation in the shallow mantle lithosphere. Journal of Petrology 51. http://dx.doi.org/10.1093/petrology/egp087.
Niida, K., 1997. Mineralogy of MARK peridotites: replacement through magma channeling examined from hole 920D, MARK area. In: Karson, J.A., Cannat, M., Miller, D.J., Elton, D. (Eds.), Proceedings of the Ocean Drilling Program, Scientific Results, vol. 153. Ocean Drilling Program, College Station, TX, pp. 265–275.
Obata, M., 1980. The Ronda peridotite: garnet, spinel and plagioclase–lherzolite facies and the p–t trajectories of a high-temperature mantle intrusion. Journal of Petrology 21, 533–572.
Operta, M., Pamić, J., Balen, D., Tropper, P., 2003. Corundum-bearing amphibolites from the metamorphic basement of the Krivaja–Konjuh ultramafic massif (Dinaride ophiolite zone, Bosnia). Mineralogy and Petrology 77, 287–295.
Pamić, J., Tomljenović, B., Balen, D., 2002. Geodynamic and petrogenetic evolution of Alpine ophiolites from the central and NW Dinarides: an overview. Lithos 65, 113–142.
Piccardo, G.B., Vissers, R.L.M., 2007. The pre-oceanic evolution of the Erro-Tobbio peridotite (Voltri massif, Ligurian Alps, Italy). Journal of Geodynamics 43, 417–449. http://dx.doi.org/10.1016/j.jog.2006.11.001.
Piccardo, G.B., Zanetti, A., Müntener, O., 2007. Melt/peridotite interaction in the southern Lanzo peridotite: field, textural and geochemical evidence. Lithos 94, 181–209. http://dx.doi.org/10.1016/j.lithos.2006.07.002.
Putirka, K., Johnson, M., Kinzler, R., Longhi, J., Walker, D., 1996. Thermobarometry of mafic igneous rocks based on clinopyroxene-liquid equilibria, 0–30 kbar. Contributions to Mineralogy and Petrology 123, 92–108.
Rampone, E., Piccardo, G.B., 2000. The ophiolite–oceanic lithosphere analogue: new insights from the Northern Apennines (Italy). In: Dilek, Y., Moores, E.M., Elthon, D., Nicolas, A. (Eds.), Ophiolites and Oceanic Crust: New Insights from Field Studies and the Ocean Drilling Program, vol. 349. Geological Society of America, pp. 21–34 (of Special Papers).
Rampone, E., Piccardo, G., Vannucci, R., Bottazzi, P., Ottolini, L., 1993. Subsolidus reactions monitored by trace element partitioning: the spinel- to plagioclase-facies transition in mantle peridotites. Contributions to Mineralogy and Petrology 115, 1–17.
Rampone, E., Piccardo, G.B., Vannucci, R., Bottazzi, P., 1997. Chemistry and origin of trapped melts in ophiolitic peridotites. Geochimica et Cosmochimica Acta 61, 4557–4569.
Rampone, E., Piccardo, G.B., Hofmann, A.W., 2008. Multi-stage melt-rock interaction in the Mt. Maggiore (Corsica, France) ophiolitic peridotites: microstructural and geochemical evidence. Contributions to Mineralogy and Petrology 156, 453–475.
Robertson, A., Karamata, S., 1994. The role of subduction–accretion processes in the tectonic evolution of the mesozoic Tethys in Serbia. Tectonophysics 234, 73–94.
Robertson, A., Karamata, S., Šarić, K., 2009. Overview of ophiolites and related units in the late palaeozoic–early cenozoic magmatic and tectonic development of Tethys in the northern part of the Balkan region. Lithos 108, 1–36.
Schmid, S.M., Bernoulli, D., Fügenshuh, B., Matenco, L., Schefer, S., Schuster, R., Tischler, M., Ustaszewski, K., 2008. The Alpine–Carparthian–Dinaric orogenic system: compilation and evolution of tectonic units. Swiss Journal of Geosciences 101, 139–183.
Schroeder, T., Cheadle, M.J., Dick, H., Faul, U., Casey, J.F., 2007. Nonvolcanic seafloor spreading and corner-flow rotation accommodated by extensional faulting at 15°n on the mid-Atlantic ridge: a structural synthesis of odp leg 209. Geochemistry, Geophysics, Geosystems 8, Q06015. http://dx.doi.org/10.1029/2006GC001567.
Šegvić, B., 2010. Petrologic and Geochemical Characteristics of the Krivaja–Konjuh Ophiolite Complex (NE Bosnia and Herzegovina): Petrogenesis and Regional Geodynamic Implications. Ph.D. thesis Ruprecht-Karls-Universität Heidelberg.
Seyler, M., Bonatti, E., 1994. Na, Ai^{IV} and Ai^{VI} in clinopyroxenes of subcontinental and suboceanic ridge peridotites: a clue to different melting processes in the mantle? Earth and Planetary Science Letters 122, 281–289.
Seyler, M., Bonatti, E., 1997. Regional-scale melt-rock interaction in lherzolitic mantle in the Romanche Fracture Zone (Atlantic Ocean). Earth and Planetary Science Letters 146, 273–287.
Seyler, M., Cannat, M., Mével, C., 2003. Evidence for major-element heterogeneity in the mantle source of abyssal peridotites from the Southwest Indian Ridge (52° to 68°E). Geochemistry, Geophysics, Geosystems 4, 9101. http://dx.doi.org/10.1029/2002GC000305.
Seyler, M., Lorrand, J.P., Dick, H.J.B., Drouin, M., 2007. Pervasive melt percolation reactions in ultra-depleted refractory harzburgites at the Mid-Atlantic Ridge, 15°20′N: ODP hole 1274A. Contributions to Mineralogy and Petrology 153, 303–319. http://dx.doi.org/10.1007/s00410-006-0148-6.
Smith, A.G., 1993. Tectonic significance of the Hellenic–Dinaric ophiolites. In: Prichard, H.M., Alabaster, T., Harris, N.B.W., Neary, C.R. (Eds.), Magmatic Processes and Plate Tectonics. Geological Society Special Publication, vol. 76, pp. 213–243.
Smith, A.G., Spray, J.G., 1984. A half-ridge transform model of the Hellenic–Dinaric ophiolites. In: Dixon, J.E., Robertson, A. (Eds.), The geological evolution of the Eastern Mediterranean. Geological Society Special Publications, vol. 17. Blackwell Scientific Publications, pp. 629–644.

Soustelle, V., Tommasi, A., Bodinier, J.L., Garrido, C.J., Vauchez, A., 2009. Deformation and reactive melt transport in the mantle lithosphere above a large-scale partial melting domain: the Ronda peridotite massif, southern Spain. Journal of Petrology 50, 1235–1266. http://dx.doi.org/10.1093/petrology/egp032.

Suhr, G., Hellebrand, E., Johnson, K., Brunelli, D., 2008. Stacked gabbro units and intervening mantle: a detailed look at a section of IODP Leg 305, Hole U1309D. Geochemistry, Geophysics, Geosystems 10. http://dx.doi.org/10.1029/2008GC002012.

Tartarotti, P., Susini, S., Nimis, P., Ottolini, L., 2002. Melt migration in the upper mantle along the Romanche Fracture Zone (Equatorial Atlantic). Lithos 63, 125–149.

Tuff, J., Takahashi, E., Gibson, S.A., 2005. Experimental constraints on the role of garnet pyroxenite in the genesis of high-Fe mantle plume derived melts. Journal of Petrology 46, 2023–2058.

Ustaszewski, K., Kounov, A., Schmid, S.M., Schaltegger, U., Krenn, E., Frank, W., Fgenschuh, B., 2010. Evolution of the AdriaEurope plate boundary in the northern Dinarides: from continentcontinent collision to backarc extension. Tectonics 29, TC6017. http://dx.doi.org/10.1029/2010TC002668.

van der Wal, D., Vissers, R.L.M., 1996. Structural petrology of the Ronda peridotite, sw Spain: deformation history. Journal of Petrology 37, 23–43.

van der Wal, D., Chopra, P., Drury, M., Fitz Gerald, J.D., 1993. Relationships between dynamically recrystallized grain size and deformation conditions in experimentally deformed olivine rocks. Geophysical Research Letters 20, 1479–1482.

Warren, J.M., Hirth, G., 2006. Grain size sensitive deformation mechanisms in naturally deformed peridotites. Earth and Planetary Science Letters 248, 438–450.

Witt-Eickschen, G., O'Neill, H.S., 2005. The effect of temperature on the equilibrium distribution of trace elements between clinopyroxene, orthopyroxene, olivine and spinel in upper mantle peridotite. Chemical Geology 221, 65–101. http://dx.doi.org/10.1016/j.chemgeo.2005.04.005.

Workman, R.R., Hart, S.R., 2005. Major and trace element composition of the depleted MORB mantle (DMM). Earth and Planetary Science Letters 231, 53–72. http://dx.doi.org/10.1016/j.epsl.2004.12.005.